

AD-A034 019 AIR FORCE INST OF TECH WRIGHT-PATTERSON AFB OHIO SCH--ETC F/6 18/3  
RESIDUAL SIGNATURES FROM THERMONUCLEAR AIR BURSTS. (U)  
DEC 76 G E KELLY

UNCLASSIFIED

ONE/PH/760-5

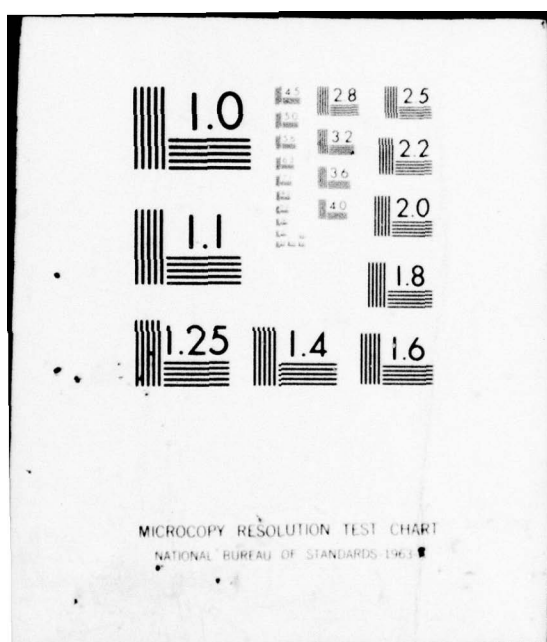
NL

| OF |  
AD  
A034019

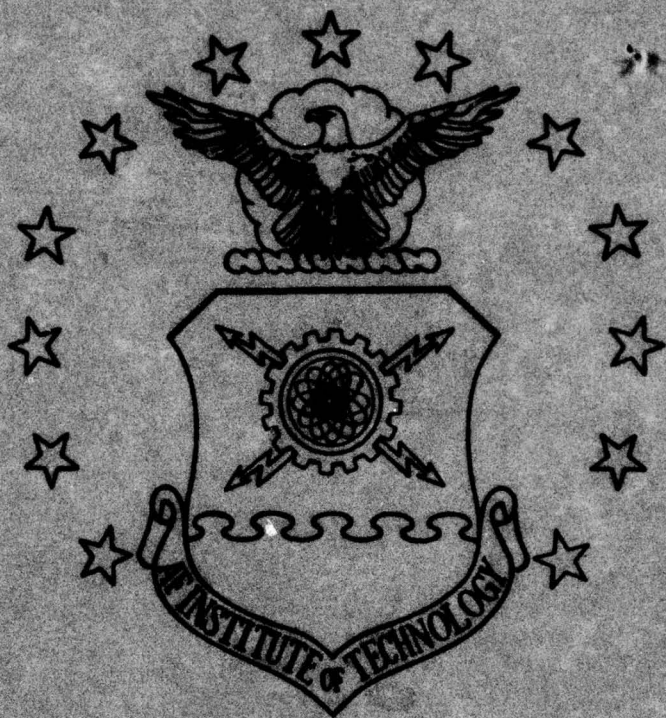


END

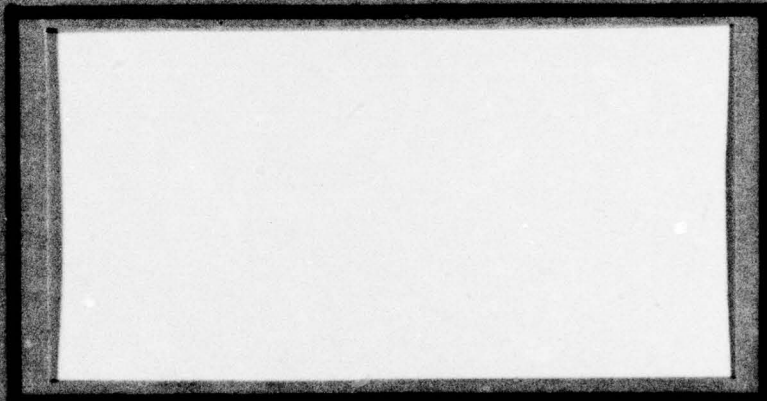
DATE  
FILMED  
2-77



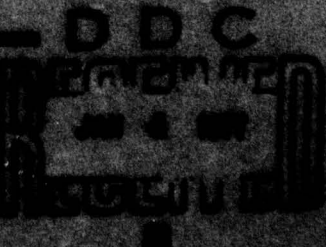
ADA034019



8  
doc  
1



UNITED STATES AIR FORCE  
AIR UNIVERSITY  
AIR FORCE INSTITUTE OF TECHNOLOGY  
Wright-Patterson Air Force Base, Ohio



9 Master's thesis,

6 RESIDUAL SIGNATURES FROM  
THERMONUCLEAR AIR BURSTS

THESIS

14 GNE/PH/76D-5

10 Gordon E. Kelly  
Capt. USAF

11 Dec 76

12 75p.

ACCESSION FOR	
NTIS	White Section
DOC	Buff Section <input type="checkbox"/>
UNANNOUNCED	
JUSTIFICATION	
BY	
DISTRIBUTION/AVAILABILITY CODES	
ORIG.	AVAIL. and/or SPECIAL
A	

Approved for public release; distribution unlimited

dr  
012 225

RESIDUAL SIGNATURES FROM  
THERMONUCLEAR AIR BURSTS

THESIS

Presented to the Faculty of the School of Engineering  
of the Air Force Institute of Technology  
Air University  
in Partial Fulfillment of the  
Requirements for the Degree of  
Master of Science

by

Gordon E. Kelly, B.S.

Capt. USAF

Graduate Nuclear Engineering

December 1976

Approved for public release; distribution unlimited

Preface

The purpose of this study was to determine if a specific thermo-nuclear weapon, detonated at such a height as to preclude crater formation, would leave a signature which would remain distinguishable for up to approximately 13 hours. Primary consideration was given to thermal ground heating.

I would like to thank Dr. Charles J. Bridgman, of AFIT, for his support and guidance. Major Brian G. Stephan, SAC/XPFS, the thesis sponsor, is due thanks for his support and invitation to discussions with contractors studying the DA/S problem.

I am also indebted to Dr. Gerhard Rohringer, of the General Research Corporation, who supplied me with material which supports the accuracy of my thermal heating model.

Gordon E. Kelly

## Contents

	Page
Preface .....	ii
List of Figures .....	v
List of Tables .....	vi
Abstract .....	vii
I. Introduction .....	1
Purpose .....	1
Definition of Terms .....	1
Background .....	2
Assumptions .....	3
II. Prompt Thermal Heating About Ground Zero .....	4
Analytic Solution .....	5
Finite Difference Solution .....	7
III. Fission Product Heating .....	16
Heat Generation by Fission Products .....	17
Spherical Divergence of Fission Fragments .....	18
Signature Alteration by Fallout .....	19
IV. Gamma Activity from Neutron Activated Soil .....	21
$^{24}$ Flux from $\text{Na}^{24}$ Gammas .....	23
Extraneous Fission Product Gammas .....	26
V. Conclusions .....	29
Bibliography .....	32
Appendix A: Thermo-physical Properties of Soil Types and References .....	34
Appendix B: Thermal Flux Inputs for HTET4 .....	36
Appendix C: Space-Time Mesh for HTET4 .....	38
Appendix D: Differenced Heat Conduction Equation and Newton-Raphson Treatment of the Surface Temperature .....	40
Appendix E: Computer Program HTET4 .....	44
Flow Chart .....	45
Glossary .....	52
Listing .....	54

<b>Appendix F: Computer Program HTE5 .....</b>	<b>61</b>
<b>Glossary .....</b>	<b>61</b>
<b>Listing .....</b>	<b>62</b>
<b>Appendix G: DA/S Sortie-Neutron Activation Geometry .....</b>	<b>64</b>
<b>Vita .....</b>	<b>65</b>

List of Figures

<u>Figure</u>	<u>Page</u>
1 Insulated Surface Temperature of the Earth from Prompt Thermal Heating .....	6
2 Surface Temperature Increase in the Earth from 10 to 1000 sec after Detonation, Produced by Prompt Thermal Radiation .....	10
3 Surface Temperature Increase in the Earth from 1000 to 50,000 sec after Detonation .....	11
4 Distribution of Above Ambient Temperatures into the Earth at Various Times after Detonation .....	12
5 Neutron-Induced Gamma Flux as a Function of Altitude and Distance from Ground Zero .....	25
6 Percent of Thermal Energy Emitted as a Function of Time Since Detonation .....	36
7 Thermal Flux Input Spectrum: HTE4 .....	37
8 Newton-Raphson Sliding Tangent .....	42
9 DA/S Sortie-Neutron Activation Geometry .....	64

## List of Tables

### Table

I	Surface Temperature Increase at Four and Thirteen Hours, Produced by Prompt Thermal Heating .....	10
II	Soil Constituents Used in the Analysis of Neutron Activation .....	21
III	Comparison of the ORNL-4464 $4\text{mr}^2$ Scalar Flux and the Approximation Thereto .....	23
IV	Potentially Troublesome Fission Product Gammas .....	26
V	Fractional Flux at Various Altitudes .....	28
VI	Thermo-physical Properties of Six Soil Types .....	34
VII	Soil Type Common Names and References .....	35
VIII	Spatial Mesh: HTE <sup>4</sup> .....	38
IX	Time Mesh: HTE <sup>4</sup> .....	39

Abstract

Prompt thermal heating of the ground, fission product deposition, and neutron activation of soil were studied as possible indicators of nuclear weapon damage levels. The time of interest was the period of approximately thirteen hours following a 500 KT low altitude, non-cratering burst.

A computer model was constructed to calculate the distribution of weapon-induced temperature increases within the earth. Surface thermal signatures at four hours were detectable and ranged up to  $11\text{ K}^{\circ}$  above ambient. The signature had decayed to background levels by 13 hours.

Fission product heating was determined to be unusable as an indicator of a weapon's ground zero. Fission products, deposited in high concentrations on the earth's surface as from severe rainout, may alter the early thermal signatures through beta particle induced ground heating. Calculated temperature increases for severe rainout ranged up to  $35\text{ K}^{\circ}$ .

Neutron induced activity, for a given soil, was calculated using approximations to the ORNL-4464  $4\text{mr}^2$  scalar flux. Activation of a thin layer at the earth's surface was assumed. The integrated gamma flux from  $\text{Na}^{24}$  at 13 hrs after detonation was calculated for various altitudes and ground distances from the ground zero. Values over ground zero ranged from  $8.50 \times 10^5 \gamma/\text{s/cm}^2\text{sec}$  at an altitude of 100 ft to  $1.02 \times 10^4$  at 1500 ft altitude. At a ground range of 10,000 ft the integrated flux was  $32 \gamma/\text{s/cm}^2\text{sec}$  at an altitude of 100 ft. A list of fission product gammas which could mask or confuse this signature was compiled.

RESIDUAL SIGNATURES

FROM

THERMONUCLEAR AIR BURSTS

I. Introduction

Purpose

This study was performed to determine if a weapon whose height of burst (HOB) precludes crater formation leaves a detectable residual signature. The reference weapon is a 500 KT thermonuclear device having a 250 KT fission yield. It is detonated at an HOB of 5000 ft above ground level. Preference was given to the possible detection of thermal signatures by state-of-the-art airborne infrared sensors. However, the study was not restricted from suggesting different systems. The time frame of interest for residual signatures lasts for up to approximately 13 hrs.

Definition of Terms

In this report "early times" refers to times up to detonation plus four hours. "Early-time signatures" refers to signatures from weapon-related phenomena at approximately four hours. "Late times" exist from after the four-hour point until detonation plus approximately 13 hrs. "Late-time signatures" are those at approximately the 13-hr point.

"Fission fragments" are isotopes produced by fission of the weap-

on's fissile material. The term "fission products" denotes the aggregation of fission fragments and all subsequent daughters.

"Ground zero" is that point, on the earth's surface, which directly underlies the burst point.

#### Background

A damage assessment/strike (DA/S) sortie could be flown against a previously attacked target as insurance of target destruction. In a general nuclear war, a certain number of aircraft could be assigned missions of this type and would be designated DA/S sorties.

While inbound to the target, the crew of a DA/S sortie would have to determine if the objective had been destroyed. If the crew could determine that the actual ground zero (AGZ) was within a certain range of the target, the target would be assumed to have been destroyed. Weapons assigned to a target lying within the specified radius from the AGZ would not be released. If the target was outside the radius, the target would be struck as planned.

In some cases, targeting constraints might require that certain allocated weapons be detonated at an HOB which does not allow crater formation. Such conditions might not produce usable visual or radar indications of the weapon's ground zero. If DA/S tactics could be applied to these cases, destruction could be assured without the needless expenditure of valuable weapons. Acceptable solutions to this problem are limited by the practical considerations of a DA/S sortie in a general nuclear war environment. A DA/S aircraft approaches its target at high speed and low altitude. The decision to strike or withhold weapon release must be made while inbound to the target on the bomb run.

Multiple approaches to the target are not feasible. Decision-making information must be quickly and easily obtainable while the decision making algorithm is kept simple.

Assumptions

In this study the earth was assumed to be flat and infinite in depth and breadth. It is thus termed semi-infinite. It was assumed that the earth's surface absorbed all incident phenomena. Absorption was allowed in a thin layer at the earth's surface. Heat was transferred into the earth by conduction only. The earth's thermo-physical properties were not allowed to change while the phenomena under study were occurring.

The fireball was considered to be a point source for thermal output calculations. Firestorm conflagrations were not considered. All heat related assumptions were made so as to maximize the absorption and retention of heat by the earth. Prompt thermal heating calculations exclude the relatively small contributions from shock, neutron, and gamma heating of the surface.

## II. Prompt Thermal Heating About Ground Zero

A nuclear weapon, detonated near the earth's surface, may have as much as 44% of its total energy manifested as prompt thermal radiation (Ref 1:24). This radiation arises when the weapon's soft X-radiation ( $h\nu \leq 20$  keV) is absorbed by the air within a few feet of the detonation point. The absorption heats the surrounding air and forms the characteristic fireball which radiates at several thousand  $^{\circ}\text{C}$  for much of its life. The fireball emits characteristic blackbody radiation having wavelengths primarily in the ultraviolet, visible, and infrared portions of the spectrum. This radiation, emitted by the fireball in the first minute or less, is termed prompt thermal radiation (Ref 2:26, 75,317). The total prompt thermal radiation or thermal fluence,  $F$ , incident on a target is

$$F = WfT/4\pi R^2 \quad (\text{cal/cm}^2) \quad (1)$$

where:

$W$  = weapon's explosive yield in calories

$f$  = thermal fraction (fraction of the yield which manifests itself as prompt thermal radiation)

$T$  = atmospheric transmittance ( $T \leq 1$ )

$R$  = distance from burst point to target (cm).

To determine if a residual signature would exist at ground zero, the fluence at this point was computed, and that value was assumed to be uniformly distributed over a semi-infinite earth such that  $F$  calories were deposited on and absorbed by each square cm of surface. The temperature distribution in time and space may be calculated from a solution to the general, one-dimensional heat conduction equation (Ref 3:11):

$$\frac{\partial T(x,t)}{\partial t} = \frac{k}{\rho c} \frac{\partial^2 T(x,t)}{\partial x^2} \quad (2)$$

where:  $T(x,t)$  = temperature in  $^{\circ}\text{K}$  at depth  $x$  and time  $t$   
 $k$  = thermal conductivity (cal/cm sec  $^{\circ}\text{K}$ )  
 $\rho$  = density of soil (gm/cm $^3$ )  
 $c$  = specific heat (cal/gm  $^{\circ}\text{K}$ ).

The general boundary conditions are

$$Q(0,t) = Q_{ab} - Q_{cv} - Q_{rr} = -k \left[ \frac{\partial T(x,t)}{\partial x} \right]_{x=0} \quad (3)$$

where:  $Q(0,t)$  = net rate of heat flow at the surface (cal/cm $^2$  sec)  
 $Q_{ab}$  = rate of heat absorption  
 $Q_{cv}$  = rate of convection from surface to air  
 $Q_{rr}$  = rate of re-radiation by the surface.

At great depths the change in temperature is negligible. Since the deposition of heat on the surface is assumed to be uniform and infinite in extent, no heat flow occurs in the horizontal plane.

#### Analytic Solution to the Heat Conduction Equation

As a limiting case, the total fluence was assumed to have been delivered as a delta function in time. The earth's surface was taken to be insulated with the exception of the fluence input. Thus, predicted temperatures will be unrealistically high. With these limitations Eq (3) becomes

$$Q(0,t) = -k \left[ \frac{\partial T(x,t)}{\partial x} \right]_{x=0} = F\delta(t). \quad (4)$$

With these restrictions imposed, Eq (2) is solvable in closed form by the method of Laplace transforms. The solution is

$$T(x,t) = \frac{F}{k} \sqrt{\alpha/\pi t} e^{-x^2/4\alpha t} \quad (5)$$

where  $\alpha = k/\rho c$  is the thermal diffusivity with units of  $(\text{cm}^2/\text{sec})$ . By Eq (1) a 500 KT weapon, having a thermal fraction of 0.43, if detonated at 5000 feet above ground level in an atmosphere whose transmittance is 0.95, will deposit a total of  $700 \text{ cal/cm}^2$  at ground zero. Fig. 1 is a plot of Eq (5) for three representative types of soil. Curve I is for sandy clay, which is soil type I. Curve V is for very dry soil, and curve VI is for wet mud, which are soil types V and VI respectively. The thermo-physical properties and common names of the six soil types considered in this study are listed in Appendix A.

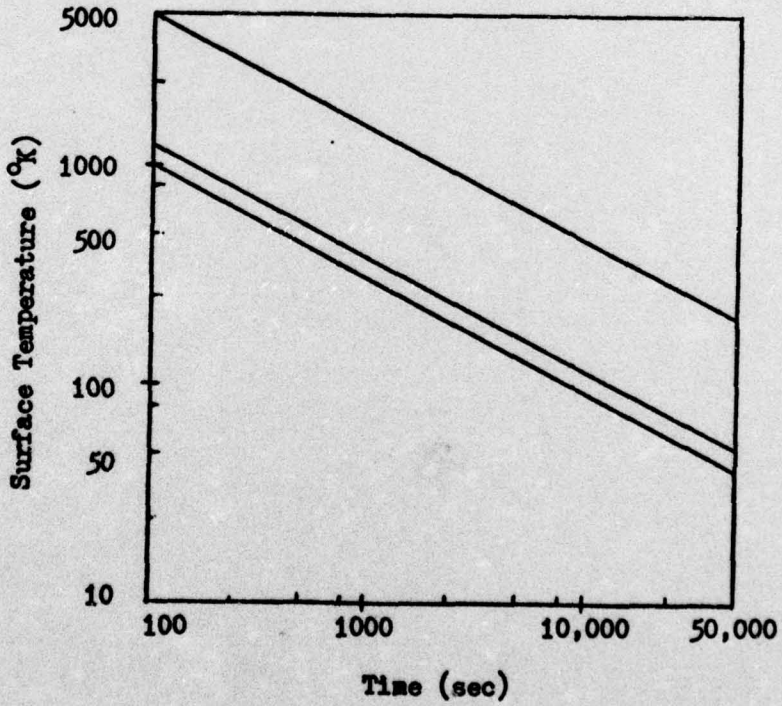


Fig. 1. Insulated Surface Temperature

The conduction of heat into the earth was slow enough to allow high residual surface temperatures to exist at late times.

The effects of convection and re-radiation were considered next. The earth's surface was assumed to radiate according to Stefan's law (Ref 4:48):

$$Q_{rr} = \sigma \epsilon T_s^4 \quad (\text{cal/cm}^2 \text{sec}) \quad (6)$$

where:

$\sigma$  = Stefan-Boltzman constant ( $\text{cal/cm}^2 \text{sec}^{-1} \text{K}^4$ )

$\epsilon$  = emissivity of the surface (unitless)

$T_s$  = surface temperature ( $^{\circ}\text{K}$ )

Free convection, assumed to take place at the surface, was taken to be

$$Q_{cv} = h T_s \quad (\text{cal/cm}^2 \text{sec}) \quad (7)$$

where  $h = 2.98 \times 10^{-5} T_s^{0.33}$  ( $\text{cal/cm}^2 \text{sec}^{-1} \text{K}^{0.33}$ ) (Ref 5:180,444). With the addition of these terms to the surface boundary condition, an analytic solution to the heat conduction equation was no longer possible. The method of finite differences was employed to obtain solutions at a finite number of points.

#### Finite Difference Solution to the Heat Conduction Equation

A computer solution to the prompt thermal problem also allowed the input fluence to be distributed as a flux in time. The standard thermal fluence spectrum was modified to allow for 100% of the 500 KT weapon's prompt thermal yield to be delivered in ten seconds. This modified spectrum and the flux input spectrum are contained in Appendix B. For the case under study, the most rapid change in thermal output occurs in

the first two seconds of yield generation. The largest time interval of this two second period, over which the change in output was nearly linear, was chosen as the flux input time-interval. It was found that for intervals shorter than 0.1 sec, the late-time temperatures did not vary significantly. This value of the input time interval required 500,000 time levels to extend the calculations to 13 hrs. A graded time mesh, having a maximum interval of five seconds, was used to shorten the calculation time. To further shorten the calculation time a graded spatial mesh was employed. It consisted of 35 nodes with  $\Delta x$  varying from 0.2 cm, near the surface, to 10 cm at depths beyond 50 cm. The graded space-time grid is described in greater detail in Appendix C.

The heat conduction equation, Eq (2), was differenced using a second central difference approximation to the spatial derivative and a first forward difference approximation to the time derivative. Eq (2) becomes a four-point, two-level equation:

$$T_{i,j+1} = \beta_{1,i,j} T_{i+1,j} + (1 - \beta_{1,i,j} - \beta_{2,i,j}) T_{i,j} + \beta_{2,i,j} T_{i-1,j} \quad (8)$$

where:  $T_{i,j}$  = temperature of the  $(i,j)^{\text{th}}$  mesh point

$$\beta_{1,i,j} = 2\alpha\Delta t_j / (\Delta x_i \Delta x_{i+1} + \Delta x_{i+1}^2)$$

$$\beta_{2,i,j} = 2\alpha\Delta t_j / (\Delta x_i^2 + \Delta x_i \Delta x_{i+1})$$

$\Delta x_i$  = distance from the  $(i-1)^{\text{th}}$  spatial node to the  $i^{\text{th}}$

$\Delta t_j$  = distance between time node  $j$  and  $(j+1)$ .

For space-time stability, both  $\beta_{1,i,j}$  and  $\beta_{2,i,j}$  must be less than 0.5.

A complete derivation of Eq (8) is in Appendix D. The surface boundary condition, Eq (3), in differenced form is

$$Q(0,t) = -k \frac{T_{2,j} - T_{1,j}}{\Delta x_1} \quad (9)$$

and an application of the Newton-Raphson technique, described in Appendix D, provides the surface temperature at time level  $j$ :

$$T_{n+1} = \frac{3C_1 T_n^4 + C_2 (9.93 \times 10^{-6}) T_n^{1.33} + C_2 TFLX + T_2}{4C_1 T_n^3 + C_2 (3.97 \times 10^{-5}) T_n^{0.33} + 1} \quad (10)$$

where:

$$C_1 = \Delta x_1 \sigma / k$$

$$C_2 = \Delta x_1 / k$$

$T_{n+1}$  =  $(n+1)^{th}$  iteration of the surface temperature  
at time level  $j$

TFLX = weapon's thermal flux input into the earth at  
time level  $j$

$T_2$  = temperature of the first subsurface node at  
time level  $j$

The computer program listed in Appendix E was assembled to calculate the change in the earth's temperature as a function of time. The program, referred to as HTE<sup>4</sup>, can be used to calculate temperature distributions up to 50,000 sec (13.9 hrs) after detonation.

The following results are the temperature increases produced in soil types I through VI by the 500 KT standard weapon. Table I lists the surface temperatures, rounded to the nearest half degree, at four and thirteen hours after detonation for the six soil types listed in Appendix A.

Table I  
Surface Temperature Increase at 4 and 13 Hours

Soil Type	Temperature (K°)	
	4 hrs	13 hrs
I	11.5	5.0
II	7.0	3.0
III	6.5	2.5
IV	10.0	4.5
V	4.5	1.5
VI	10.0	5.0

Surface temperature increases for soil types I, II, and V are displayed in Fig. 2 from 10 sec to 1000 sec after detonation.

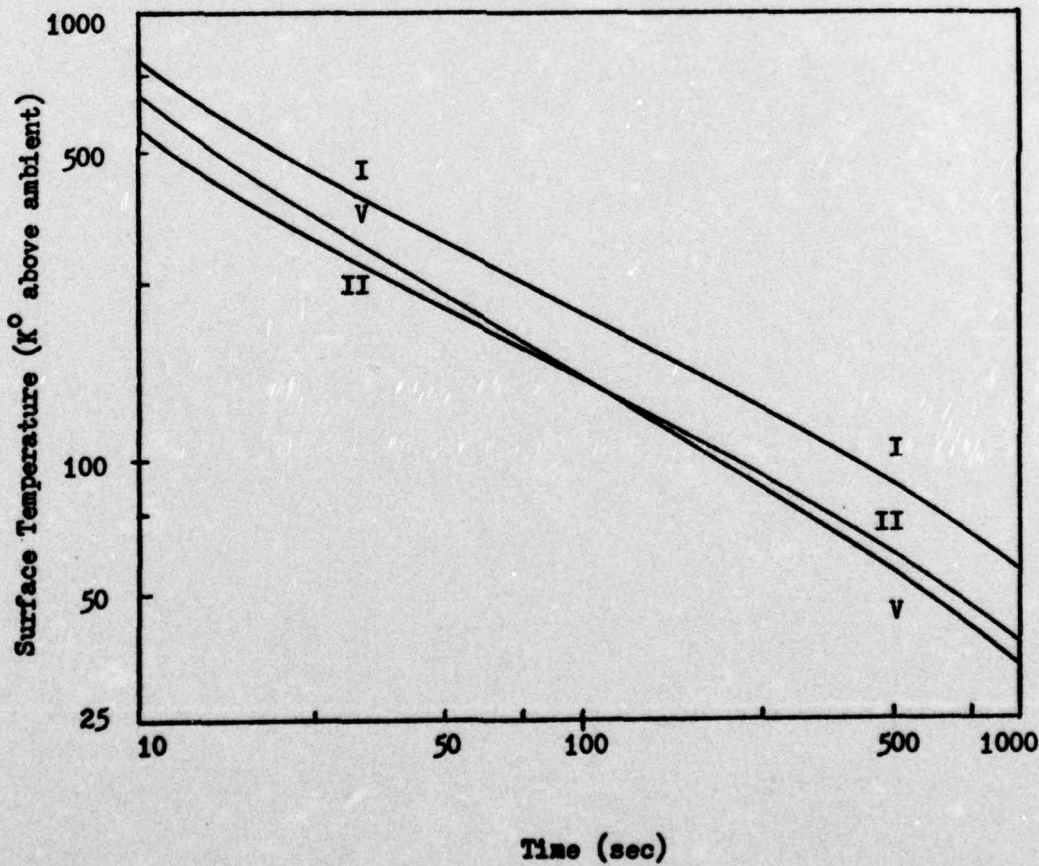


Fig. 2 Surface Temperature Increase from 10 sec to 1000 sec

Figure 3 is a plot for soil types I, II, and V from 1000 sec to 50,000 sec. Note that the addition of convection and re-radiation at the surface has reduced the late-time temperature of soil type V from the highest value in Fig. 1 to the lowest in Fig. 3.

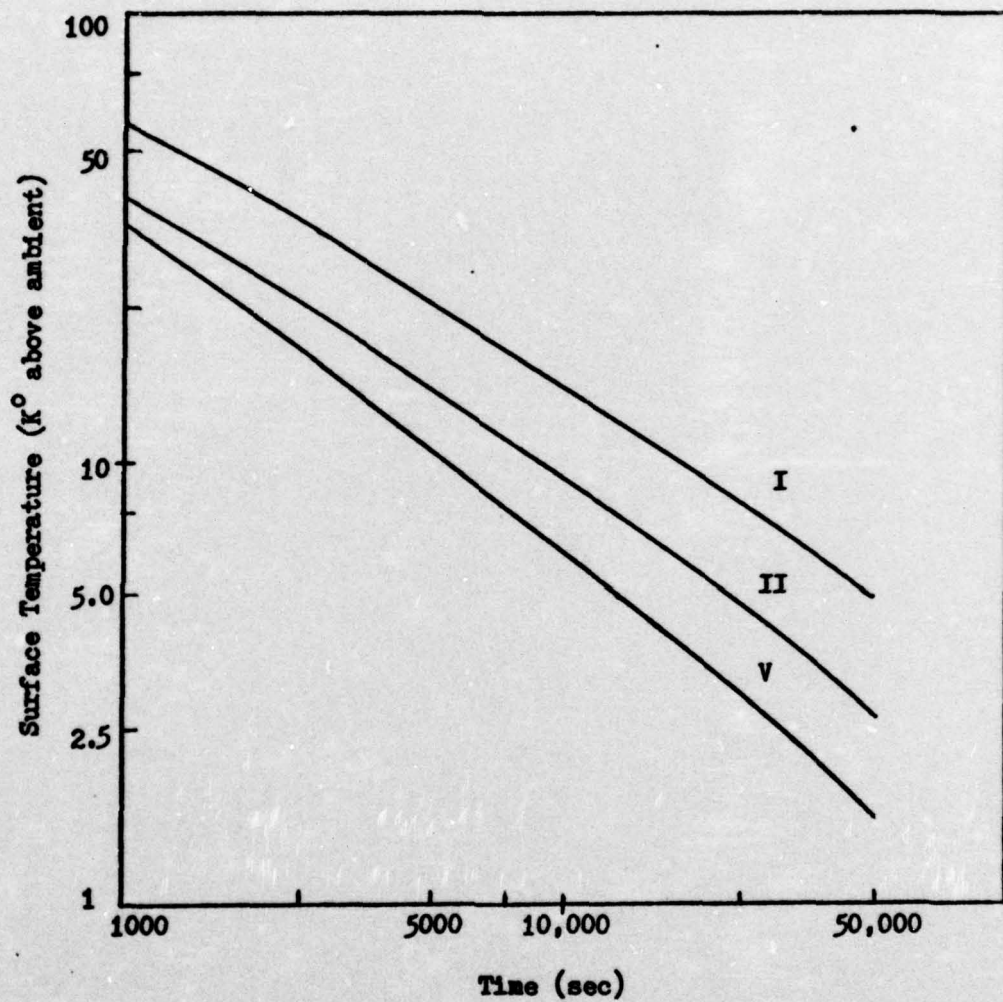


Fig. 3. Surface Temperature Increase from 1000 to 50,000 sec

Figure 4 illustrates the temperature distribution into soil type I at various times after detonation. The three plots are for 10 sec, 100 sec, and 1000 sec elapsed times. The effects of both conduction and surface heat removal phenomena are evident.

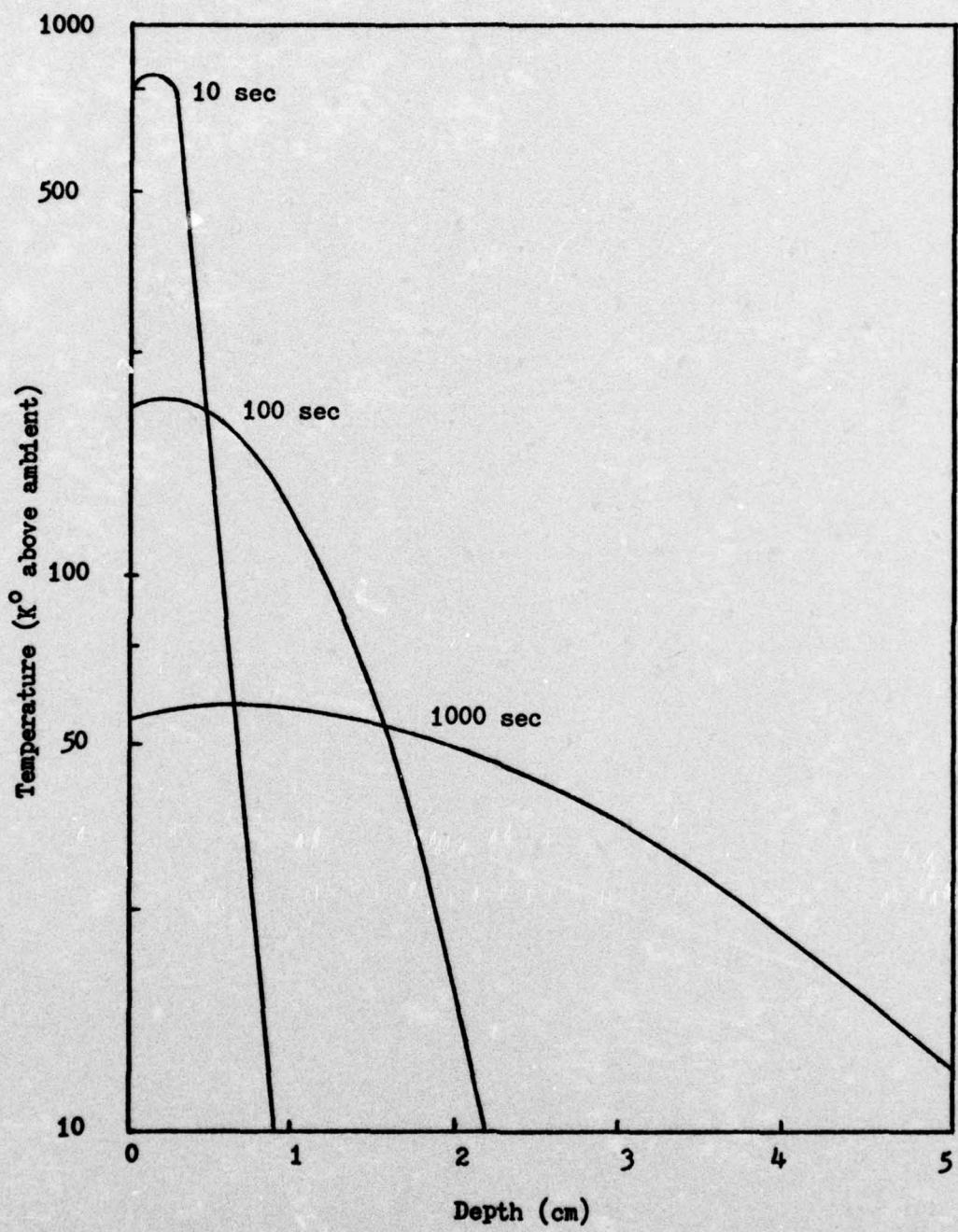


Fig. 4. Distribution of Above Ambient Temperatures  
into Soil Type I

The value used for the surface emissivity was unity. Actual emissivity values may range from 0.8 to 0.95 depending on the surface covering. The use of a value of 0.80 instead of 1.00, in HTE4, increased both early and late-time temperatures by about 4%. For soil type VI this was the equivalent of approximately  $0.4\text{ K}^{\circ}$  at four hours and  $0.2\text{ K}^{\circ}$  at thirteen hours. For the same soil, a 20% error in the re-radiation term produced temperature differences of  $200\text{ K}^{\circ}$  during the flux input period. This difference decreased to less than  $0.2\text{ K}^{\circ}$  at late times.

Surface temperature differences caused by convection term differences of 20% or less were negligible shortly after detonation when re-radiation dominates the heat transfer processes. At late times, a 20% difference in the convection term produced a calculated surface temperature which differed from the given value by up to 10%.

An error in the surface temperature was induced by the calculational algorithm, of HTE4, which neglected temperature differences in the spatial mesh which were smaller than  $0.1\text{ K}^{\circ}$ . Decreasing this value to  $0.01\text{ K}^{\circ}$  increased the surface temperatures at 50,000 sec by less than 1.0%. The following inputs resulted in late-time temperature differences of three percent or less: a thermal fraction between 0.33 and 0.43, a value of the atmospheric transmittance between 0.73 and 0.95, a burst height of  $5000 \pm 500$  ft, and an input fluence error of  $\pm 20\%$ . The computer model was, therefore, relatively unaffected by errors of less than 20% in input parameters or surface loss terms.

HTE4 was used to model the Hiroshima bomb as a check on the code's accuracy. The weapon had a yield of approximately 20 KT and was detonated at an altitude of 1850 ft. The flux input was modeled according

to the constraints of Appendix B. The flux input time was limited to three seconds (Ref 2:89). The ground zero fluence calculated by Eq (1) was  $180 \text{ cal/cm}^2$ . A thermal fraction of 0.40 and a transmittance of 0.90 were used. The thermo-physical properties of firebrick were used to approximate those of clay tile (Ref 6:288). A peak surface temperature of approximately  $4000^{\circ}\text{K}$  was calculated for less than 0.2 sec. The surface temperature had decreased below  $1800^{\circ}\text{K}$  at one second after detonation. These results are in general agreement with the recorded effects at Hiroshima and subsequent tests conducted by the National Bureau of Standards (Ref 7:25).

The distribution of above-ambient temperatures into the earth, in the modeled Hiroshima weapon, did not exceed  $5^{\circ}\text{K}$  beyond a depth of five cm. This temperature increase would not have destroyed the roots of the weeds and wild flowers native to Hiroshima. According to reports, the weeds and wildflowers were flourishing about ground zero within three weeks after the explosion (Ref 8:45).

As an indication of background temperature variations, the temperatures induced by solar heating of soil types I through VI were calculated numerically. The calculational scheme was similar to the code of this section except for a constant flux input. A value of  $1.88 \times 10^{-3} \text{ cal/cm}^2\text{sec}$  was used as the solar flux absorbed by a blackened, semi-infinite earth (Ref 9:465). The temperature differences, after four hours, between soil types which could be expected to exist in the same locale were considered. The difference between types II and IV was  $4^{\circ}\text{K}$ . Types III and V varied by  $3^{\circ}\text{K}$ . For types IV and VI the difference was  $0.5^{\circ}\text{K}$ , while types I and VI varied by  $2.5^{\circ}\text{K}$ . These variations would make similar weapon-induced increases difficult

to resolve.

The stability of this model's predictions, coupled with its ability to predict values which lie within those found at Hiroshima, indicate that the surface temperatures calculated in this study are realistic. The calculated, late-time, above ambient temperature increases were generally less than 5 K<sup>o</sup>. This upper limit figure, coupled with the calculated background temperature variations, indicated that thermally produced signatures would have decayed to background level by late times. The existance of early-time signatures would be strongly dependent on soil type and the time since detonation.

### III. Fission Product Heating

By definition, no surface-fireball interaction takes place for an airburst. However, large amounts of surface debris have been observed rising into and being ejected from the top of airburst fireballs. This debris does not become highly contaminated by fission products as might be expected. Within a few seconds after detonation the fireball takes on a toroidal shape with an updraft in the center and a downdraft around the outside rim. Surface debris which is entrained upward passes along the toroid's central axis. Little mixing with the fission products contained in the toroid occurs. Experimental evidence indicates that surface material thus entrained contains negligible fallout (Ref 10:105).

For the first few seconds after detonation the bulk of a weapon's fission fragments exist as a gas or vapor due to the high core temperatures,  $T > 10^8$  °K. These gaseous and vaporized atoms are carried up by the rising fireball. As the fireball cools, the fission fragments nucleate and condense into particles with a maximum diameter of about 20 microns (Ref 11:102).

For purposes of a limiting calculation (maximum fallout), it was assumed that the weapon's fission fragments were spherically diverged from the burst point, and a ground zero concentration was calculated. The temperature increase due to beta decay was calculated and taken as an upper limit. It was decided that if this increase was negligible, then no actual signature would be detectable.

### Heat Generation by Fission Products

The rate of beta decay in a gross fission product mixture follows the Way-Wigner 1.2 law (Ref 12:1327):

$$A(\tau) = A_1 \tau^{-1.2} \quad (11)$$

where  $A_1$  is the activity at  $\tau = 1$  and  $\tau = (\text{elapsed time at } A(\tau)/\text{elapsed time at } A_1)$ . Elapsed times are measured from the instant of production. This relationship is a reasonable approximation for times greater than ten seconds after fission. In this development, the maximizing assumption was made that no decay takes place prior to 10 sec. Thus the entire production of fission fragments is present at  $t = 10$  sec ( $\tau = 1$ ). If  $\bar{E}_B$  is the average beta energy per decay, the total energy given off from all beta decays is

$$E_{\text{tot}} = \bar{E}_B \int_1^\infty A_1 \tau^{-1.2} d\tau = 5\bar{E}_B A_1 \quad (12)$$

where time is measured in units of decaseconds.

The total delayed beta energy from the fission of  $U^{235}$  or  $Pu^{239}$  is approximately  $0.044W^f$  where  $W^f$  is the fission yield in energy units (Ref 13:ch 2, p 12). The activity at time  $\tau$  is then

$$A(\tau) = (0.044W^f / 5\bar{E}_B) \tau^{-1.2} \quad (\text{B's/decasecond}) \quad (13)$$

Timofeev and Nesytov (Ref 14:3) give the B activity at one minute after weapon detonation as

$$A_B = 10^8 q \quad (\text{curies}) \quad (14)$$

where  $q$  is the TNT equivalent in tons. Values for this estimate and

those calculated by Eq (13) are within an order of magnitude of each other for values of  $\bar{E}_\beta$  between 0.3 and 1.0 MeV.

The weapon's fission fragments were assumed to be deposited on the earth's surface prior to the occurrence of any disintegrations. At  $\tau = 1$  beta decay was assumed to begin, with half the betas being absorbed by the air and half being absorbed in a thin layer at the earth's surface. Backscatter from both media was neglected, and all beta energy was assumed to manifest itself as heat. Beta heating of the air was neglected.

#### Spherical Divergence of Fission Fragments

As a limiting case of the ground-zero signature, the weapon's fission fragments were spherically diverged without other attenuation. The ground-zero concentration was used to calculate the increase in temperature due to fission-product beta absorption by a semi-infinite earth. The rate at which  $\beta$ 's were absorbed by the surface was

$$R_\beta = A(\tau)/8\pi(HOB)^2 \quad (\beta/\text{cm}^2 \text{decasecond}) \quad (15)$$

The thermal flux due to this absorption was the product of the rate of absorption and the average energy per beta:

$$TFLX = 3.50 \times 10^{-4} W_f \tau^{-1.2} / (HOB)^2 \quad (\text{cal}/\text{cm}^2 \text{sec}) \quad (16)$$

The computer routine used to calculate the temperature increases may be found in Appendix F. The earth's temperature increases were calculated in a manner similar to section I. Since the temperature gradients encountered in time and space were not severe, a constant nodal-point spacing was used in both dimensions. The time interval

used was five sec, and the spatial interval was 0.2 cm.

The differenced heat conduction equation for a constant space-time mesh is

$$T_{i,j+1} = \beta T_{i+1,j} + (1 - 2\beta) T_{i,j} + \beta T_{i-1,j} \quad (17)$$

where:  $\beta = \frac{\alpha \Delta t}{\Delta x^2} < 1/2.$

For the 250 KT fission yield weapon detonated at 5000 ft HOB, the peak temperature increase in soil type VI was 37.3 K° at ten seconds after deposition. Four hrs later this temperature had decreased to 3.5 K° and at 13 hrs it was 2.5 K°.

#### Thermal Signature Alteration by Concentrated Fallout Depositions

Early-time thermal signatures may be altered by a weapon's own fission products or those from an adjacent target. A weapon detonated in or near a severe thunderstorm could have its fission products subjected to high percentages of rainout. As an example, consider that all fission products are washed out over an area equal to the maximum cross-sectional area of the fireball. The maximum diameter is (Ref 15:319)

$$D_{\max} = 460W^{0.4} \quad (\text{ft}) \quad (18)$$

where  $W$  is the total weapon yield in KT. The resulting thermal flux from beta decay at the earth's surface is

$$TFLX = 2.58 \times 10^{-12} W_c^f T^{-1.2} / W^{0.8} \quad (\text{cal/cm}^2 \text{sec}) \quad (19)$$

where  $W_c^f$  is the fission yield in calories, and  $W$  is the total yield in KT. Calculations were made using the computer code of Appendix F for the standard weapon. The results indicated a temperature increase in soil type VI of  $35 K^{\circ}$  at four hrs. For a 50% rainout, the increase was  $19 K^{\circ}$  and for a 25% rainout it was  $10 K^{\circ}$ . These figures are not appreciably altered by the deposition time so long as it occurs within a few minutes of detonation.

Results obtained by spherical divergence of the weapon's fission fragments were negligible. This calculation was made as an upper limit. Therefore, detectable residual signatures, indicative of a weapon's ground zero, would not exist at early or late times. Calculations concerning concentrated fallout or rainout depositions indicate that such depositions may mask or alter early-time, thermally-produced, ground-zero signatures.

#### IV. Gamma Activity from Neutron Activated Soil

Neutron fluence, blast overpressure, and other prompt weapon effects are relatable through the target's range from the detonation point. The activity of specific soil isotopes formed by  $(n,\gamma)$  reactions is relatable to neutron fluence if the soil composition is known. Thus a link exists between induced soil activity and prompt weapon effects. This link may prove useful as a DA/S indicator.

Fast neutrons are rapidly thermalized in soil, with peak activity occurring two to three inches below the surface. The isotope selected as an indicator of activity must be formed in an abundance which permits measurement at DA/S altitudes at late times after formation. The choice must be made based on photon energy,  $(n,\gamma)$  cross section, half-life, and concentration. Lavrenchik lists the seven primary soil constituents shown in Table II (Ref 16:18). Some elements may not be

Table II  
Soil Constituents

Element	Si	Fe	Ca	Na	K	P	Mn
% by Wt. (gm/cc)	.74	.13	.10	.075	.07	.003	.002
Atoms/cc of Soil*	$1.5^{22}$	$1.4^{21}$	$1.5^{21}$	$2.1^{21}$	$1.1^{21}$	$6.0^{19}$	$2.2^{19}$
Isotope Formed	Si <sup>31</sup>	Fe <sup>59</sup>	Ca <sup>45</sup>	Na <sup>24</sup>	K <sup>42</sup>	P <sup>32</sup>	Mn <sup>56</sup>
$\Sigma_{\text{capt}}^{\text{(b)}}$	0.4	2.5	0.6	0.5	1.2	0.2	13

\*  $1.5^{22}$  is read  $1.5 \times 10^{22}$

common to all soil types, and composition will vary from place to place.

$\text{Ca}^{45}$  and  $\text{P}^{32}$  are beta emitters. Silicon comprises 25.7% of the earth's crust by weight, but only three percent of this is  $\text{Si}^{30}$  which captures a neutron to form  $\text{Si}^{31}$  (Ref 17:B-135). This nuclide emits a 1.26 MeV gamma only 0.07% of the time and has a short half-life of 2.6 hrs (Ref 18:10). Of the remaining constituents,  $\text{Na}^{23}$  ( $n, \gamma$ ) is the best indicator. Sodium is only the sixth most abundant element worldwide, but  $\text{Na}^{23}$  is the naturally occurring isotope.  $\text{Na}^{24}$  has a 15 hr half-life and emits a 2.75 MeV gamma during each nuclear transformation. If only those reactions indicated in Table II occur, 2.47% of the incident neutron fluence would produce  $\text{Na}^{24}$  atoms.

If all incident neutrons are absorbed in a thin layer at the earth's surface, the activity as a function of distance from the burst point,  $R_b$ , and time would be (Ref 19:189)

$$A(R_b, t) = 0.0247 F(R_b) \lambda e^{-\lambda t} \quad (\text{Na}^{24} \gamma \text{'s/sec/cm}^2) \quad (20)$$

where  $\lambda$  is the decay constant in  $\text{sec}^{-1}$ .

To determine the neutron fluence at a point on the earth's surface, a survival fraction was calculated from ORNL-4464 (Ref 20:316-317,393-395). The  $4\pi r^2$  scalar flux was calculated at 1500, 1800, 2400, 3600, and 4800 meters. From the values of the flux at these ranges, the following approximation to the  $4\pi r^2$  scalar flux was empirically obtained:

$$F_s \approx 100 e^{-4.65 \times 10^{-5} R_b} \quad (\text{neutrons/source neutron}) \quad (21)$$

This development neglected the effect of the presence of the earth's surface on the neutron field and is conservative in that respect. Table III lists the values obtained from ORNL-4464 and those calculated from Eq (21). It can be seen that the maximum variation is 14%.

Table III  
Comparison of  $4\pi r^2$  Scalar Flux and  $F_s$   
in (neutrons/source neutron)

Range $R_b$ (m)	$4\pi r^2$ scalar flux	$F_s$
1500	$1.02^{-1}$	$9.35^{-2}$
1800	$2.04^{-2}$	$2.32^{-2}$
2400	$1.63^{-3}$	$1.42^{-3}$
3600	$5.43^{-6}$	$5.37^{-6}$

The scalar flux was assumed to be isotropic. The spherically diverged, surviving, neutron fluence which is absorbed by the ground is (Ref 13:ch 2,p 50)

$$F_n(R_b) = \frac{25 S e^{-4.65 \times 10^{-5} R_b}}{4\pi R_b^2} \quad (\text{neutrons/cm}^2) \quad (22)$$

where  $S$  is the total number of neutrons given off by the weapon.

#### Flux of $\text{Na}^{24}$ Gammas Encountered by a DA/S Sortie

The 2.75 MeV gamma flux available for sensing by a DA/S sortie would be the spherically diverged, atmospherically attenuated activity integrated over all space. The flux at the point denoting the aircraft location is

$$F_\gamma = \int_{R_a=a}^{\infty} \int_{\theta=0}^{2\pi} \left[ A(R_b, t) \exp(-\mu R_a) / 4\pi R_a^2 \right] d\theta dR_a \quad (23)$$

$(\gamma/\text{s/cm}^2 \text{sec})$

where:

$a$  = aircraft altitude in cm (ALT)

$R_a$  = range variable of integration relative to  
the aircraft

$R_b$  = range variable of integration relative to  
the burst point

$\mu$  = total attenuation coefficient for the 2.75  
MeV gamma in air.

$R_b$  may be written in terms of  $R_a$  and other quantities as

$$R_b = [R_a^2 - ALT^2 + D^2 - 2(R_a^2 - ALT^2)^{1/2} D \cos(2\pi - \theta)]^{1/2} \quad (24)$$

where  $D$  is the ground distance from the point representing aircraft location to the ground zero. The geometry involved in this problem is diagrammed in Appendix G. This function was integrated numerically using the AFIT subroutine SIMPD which uses Simpson's rule to approximate a double integral. It was found that flux values were not significantly increased by increases in the upper limit on  $R_a$  beyond a value equal to  $(D^2 + ALT^2)^{1/2} + HOB$ .

Figure 5 is a plot of the gamma flux encountered 13 hrs after detonation at the altitudes indicated, for ground distances up to 10,000 ft from the ground zero. In order to put this plot in perspective, one must realize that an aircraft traveling at a ground speed of 300 knots will cover the 10,000 ft ground distance in just under 20 sec. For an aircraft traveling at 500 knots the transit time is just over 11 sec.

In a real-world situation, gamma-emitting fallout depositions could confuse a sensor if the fallout pattern were similar to activation patterns.

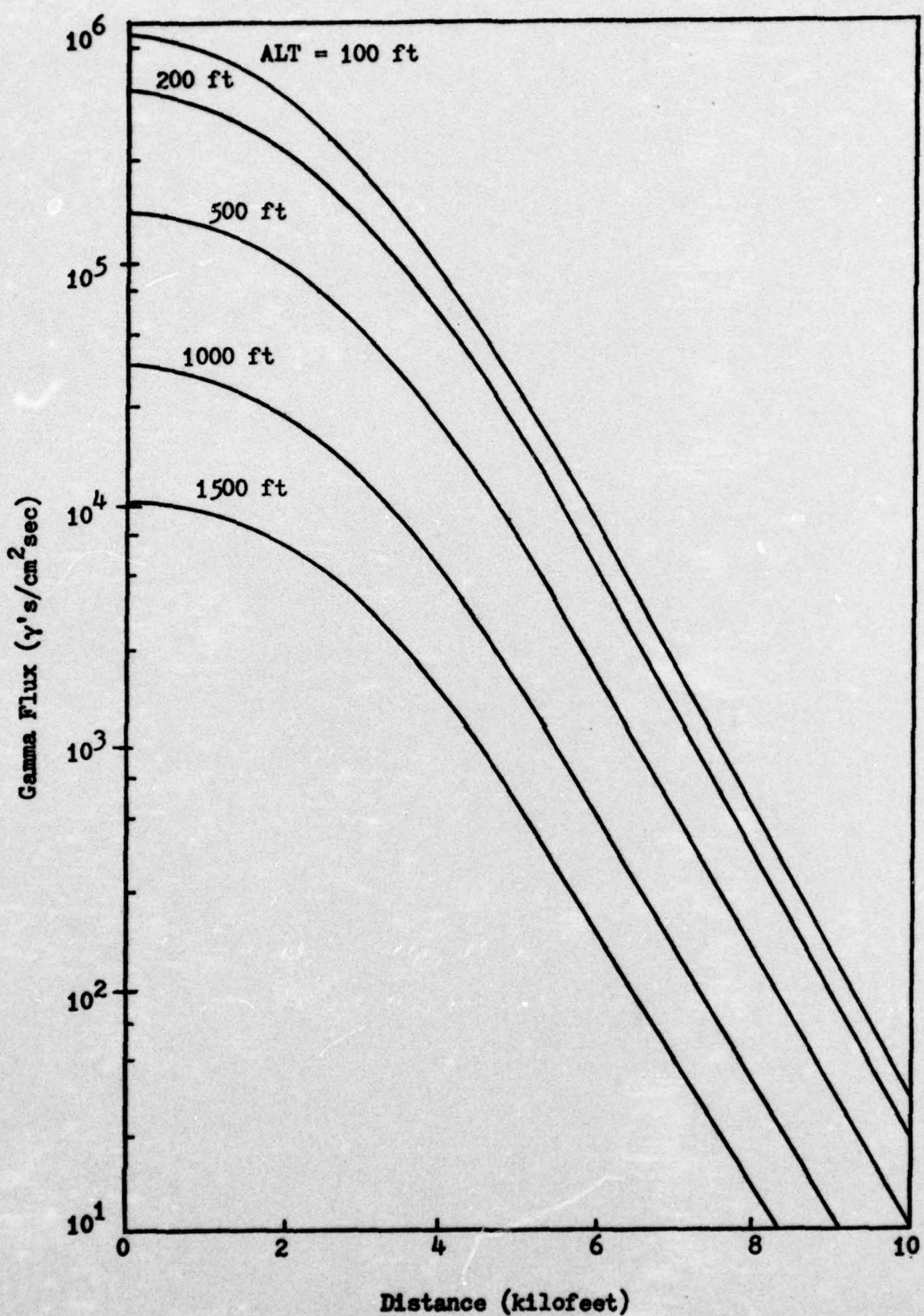


Fig. 5. Gamma flux as a function of Ground Distance at  
Detonation plus Thirteen Hours

### Extraneous Gamma Radiation from Fission Products

At one day after fission, the total gamma activity is approximately  $6.6 \times 10^6$  curies per kiloton of fission yield (Ref 16:11). Radio-nuclides which emit photons near the 2.75 MeV  $\text{Na}^{24}$  gamma were examined.

Table IV is a compilation of the fission product gammas from 250 KT of fission. Those listed have energies within 0.3 MeV of the  $\text{Na}^{24}$  gamma (Ref 18:32-82), (Ref 21:106-108), (Ref 22:87-92).

Table IV  
Potentially Troublesome Fission Product Gammas

Nuclide	Half-life	$\gamma$ Energy in MeV and (% occurrence)	Rate of Occurrence at 13 hrs After Fission ( $\gamma$ 's/sec)
$\text{Br}^{84}$	31.8 min	2.47 (8%)	$3.70^{11}$
* $\text{Kr}^{87}$	76.0 min	2.57 (35%)	$2.06^{16}$
** $\text{Rb}^{88}$	17.8 min	2.68 (2.3%)	$5.28^{16}$
$\text{Rb}^{89}$	16.0 min	2.59 (13%)	$2.57^5$
$\text{Y}^{94}$	20.0 min	2.57 (1.5%) 3.06 (1.3%)	$< 7.59^3$ $< 6.58^3$
*** $\text{Ag}^{112}$	3.2 hrs	2.55 (11%)	$4.01^{13}$
$\text{Cs}^{138}$	32.2 min	2.63 (9%)	$4.12^{12}$
$\text{La}^{140}$	40.2 hrs	2.53 (3%)	$2.18^{15}$
$\text{La}^{142}$	92.0 min	2.55 (11%) 2.99 (5%)	$7.80^{16}$ $3.55^{16}$
$\text{Pr}^{146}$	24.0 min	2.73 (1.7%)	$2.09^9$

\*  $\text{Kr}^{87}$  is the daughter of  $\text{Br}^{87}$  (56 sec)

\*\*  $\text{Rb}^{88}$  is the daughter of  $\text{Kr}^{88}$  (2.8 hrs)

\*\*\*  $\text{Ag}^{112}$  is the daughter of  $\text{Pd}^{112}$  (21 hrs)

The nuclides listed are all fission fragments except for the three indicated by asterisks.

If the weapon which produced these activities were detonated in or near severe thunderstorms, large portions of the fission product inventories would be deposited on the earth's surface. For purposes of illustration, a circular area of deposition was taken from the maximum fireball size, Eq (18). Rained-out contaminants were assumed to be uniformly distributed over this area. The flux encountered by an aircraft at an altitude of ALT would be (Ref 23:266)

$$F_e = \int_{r1}^{r2} [A \exp(-\mu R_a) / 2R_a] dR_a \quad (25)$$

where:

$r1 = ALT$

$r2 = (ALT^2 + R^2)^{1/2}$

$R$  = radius of the area of deposition

$A$  = activity per unit area

$R_a$  = range variable of integration as in Appendix G

$\mu$  = total attenuation coefficient of the gamma energy under consideration.

A value of  $5.81 \times 10^{-5} \text{ cm}^{-1}$  was used as the attenuation coefficient for all gamma energies considered ( $2.75 \pm 0.3 \text{ MeV}$ ). The flux as a function of altitude was integrated numerically with the constant  $A$  separated. The worst case was taken to be at a point over the center of the circular deposition. The results are listed in Table V in terms of the fractional flux. The flux at any altitude is the product of the fractional flux, for that altitude, and the surface activity per unit area.

$Rb^{88}$  is potentially the most troublesome gamma emitter. For a 100% fission product rainout from a 500 KT device with a 50% fission yield, the activity per unit area is  $2.37 \times 10^6 \text{ photons/cm}^2 \text{ sec}$  with

energy of 2.68 MeV. The flux as seen by an aircraft over ground zero, from Table V, would range from  $1.57 \times 10^6$  to  $2.35 \times 10^4$  gammas/cm<sup>2</sup>sec. This rate would be sufficiently high to mask signals or to confuse logic circuits designed to act on rates proportional to those shown in Fig. 5. The majority of such gammas, as described in this section, would have to be eliminated by selectively measuring the 2.75 MeV gamma and by detector characteristics.

Table V	
Fractional Flux of Fission Product Gammas at Various Altitudes	
Altitude (ft)	Fractional Flux ( $F_e/A$ )
100	.664
200	.393
500	.133
1000	.0333
1500	.0099

Neutron activation of soils would produce detectable late-time signatures. Exact knowledge of the extent of soil activation or the geometric distribution of activity would be impossible to obtain. Measurements made by a gamma detection system would be relative to a hypothetical profile as in Fig. 5. The sensing system would have to be able to evaluate all possible profiles and scan the vicinity of the target area to determine the weapon's ground zero.

## V. Conclusions

### Signatures from Prompt Thermal Radiation

The prompt thermal-heating model produced calculated temperature distributions for the Hiroshima bomb which are consistent with historically recorded facts. It was, therefore, assumed to be reasonably accurate when used for the higher yield of this study.

The residual ground-zero temperature increase for the 500 KT yield was a maximum of  $5\text{ K}^{\circ}$  at 13 hrs. For very dry soil the late-time temperature increase was only  $1.5\text{ K}^{\circ}$ . Since the heat absorbed by the earth could reasonably be expected to have a drying effect, late-time temperature increases would be in the vicinity of two to three degrees. This temperature range is below the calculated variation in background temperature which occurs due to solar heating.

Since the assumptions made tended to maximize heat retention, the values obtained must be considered maxima. Late-time thermal signatures would not be adequate or reliable as DA/S indicators. Adequate signatures would exist at early times, but the possible masking effects of thermal heating by concentrated fallout depositions from nearby bursts must be considered.

### Fission Product Heating

The assumption of spherical divergence used in the calculation of ground-zero effects was unrealistic. Most fission products in an air-burst remain in the rising fireball and subsequent cloud. In spite of this assumption, the calculated temperature increases about ground zero were negligible when compared with the calculated background variations.

Signatures produced by concentrated fission fragment fallout or rainout depositions can approximate early-time signatures from prompt thermal heating of a weapon's ground zero. This would be especially true if the deposition were graduated to heavier concentrations near the center of a circular area. A location where surface bursts also occur would be more likely to experience this effect, as early-time fallout from airbursts is negligible.

The phenomenon of ground heating by fission-product fallout leads one to consider the aerial infra-red reconnaissance of nuclear battle-fields for the purpose of locating heavy fallout depositions. Since beta and gamma activities are relatable, the heat produced by beta activity could be used to estimate the gamma activity. This could be used to estimate the potential dose to personnel entering the area.

#### Gamma Activity from Neutron Activated Soil

Calculations of the gamma flux, available for measurement by a DA/S sortie, indicate that usable signatures would exist at late times. These signatures would be measurable at altitudes and at ranges from which DA/S decisions could be made and would allow cruise missiles to be employed in a DA/S role.

The system to detect flux levels would have to be gated for the 2.75 MeV  $Na^{24}$  gamma to avoid the extraneous gammas indicated in Table IV. Due to the short reaction time available, the crew indication should be a simple go-no-go indicator. The system should employ a logic circuit to evaluate cases wherein the AGZ lies in any quadrant relative to the aircraft position at decision time.

To further refine these calculations, the effect of the earth in

the neutron field should be considered. Gamma flux based on the distribution of induced activity into the earth should be calculated. An exponential atmosphere and an attenuation coefficient which varies with it should be employed. The addition to the gamma flux by scattered photons, which lose only negligible portions of their energy, should be considered.

### Bibliography

1. DeRaad, R. G. and Meisterling, H. E. A Code for Analysis of Nuclear Effects and Systems Vulnerability. Vol. III: Blast and Thermal. Unpublished Thesis. Wright-Patterson AFB, OH: AFIT, Oct 1973.
2. Glasstone, S. (ed.) The Effects of Nuclear Weapons. Washington: USAEC, 1962.
3. Eckert, E. R. G. and Drake, R. M. Analysis of Heat and Mass Transfer. New York: McGraw-Hill, 1972.
4. Eisberg, R. M. Fundamentals of Modern Physics. New York: John Wiley, 1961.
5. McAdams, W. H. Heat Transmission (Third Edition). New York: McGraw-Hill, 1954.
6. Ingersoll, L. R. et al. Heat Conduction. Madison: University of Wisconsin Press, 1954.
7. D'Oliver, F. et al. The United States Strategic Bombing Survey: The Effects of the Atomic Bombs on Hiroshima and Nagasaki. Washington: U. S. Government Printing Office, 1946.
8. Hersey, J. "Hiroshima." The New Yorker, Aug 31, 1946. p15ff.
9. Green, A. E. S. and Wyatt, P. J. Atomic and Space Physics. Reading, Mass: Addison-Wesley, 1965.
10. Kellogg, W. W. "Atmospheric Transport and Close-In Fallout of Radioactive Debris from Atomic Explosions." The Nature of Radioactive Fallout and its Effects on Man. Pt. 1. Washington: U. S. Government Printing Office, 1957.
11. Benson, P. et al. "Physical Characteristics of Single Particles from High Yield Airbursts." Radioactive Fallout from Nuclear Weapons Tests TID 7632-Pt.1. Oak Ridge, Tn: USAEC/Division of Technical Information, Nov 1965.
12. Way, K. and Wigner, E. P. "The Rate of Decay of Fission Products." Physical Review, 73: 1318-1330, Jun 1948.
13. Bridgman, C. J. The Physics of Nuclear Explosives. Wright-Patterson AFB, OH: AFIT, 1975.
14. Timofeev, B. N. and Nesytov, Y. K. Radioactive-Contamination Forecasting. AEC-tr-7173. Jerusalem: Keter Press, 1971.
15. Eisenbud, M. Environmental Radioactivity. New York: Academic Press, 1973.

16. Lavrenchik, V. N. Global Fallout Products of Nuclear Explosions. AEC-tr-6666. Oak Ridge, Tn.: USAEC/Division of Technical Information, May 1966.
17. Weast, R. C. (ed.) Handbook of Chemistry and Physics. (Forty-seventh Edition). Cleveland: The Chemical Rubber Co., 1966.
18. Lederer, C. M. et al. Table of Isotopes. (Sixth Edition). New York: John Wiley and Sons, 1967.
19. Kaplan, I. Nuclear Physics. Reading, Ma.: Addison-Wesley, 1956.
20. Straker, E. A. and Gritzner, M. L. Neutron and Secondary Gamma-Ray Transport in Infinite Homogeneous Air. ORNL-4464. Oak Ridge, Tn.: Oak Ridge National Laboratory, Dec 1969.
21. Hyde, E. K. The Nuclear Properties of the Heavy Elements. Vol. III: Fission Phenomena. Englewood Cliffs, N. J.: Prentice-Hall, 1964.
22. Petrov, R. V. et al. Radioactive Fallout. AEC-tr-6634. Jerusalem: S. Monson, 1966.
23. Murray, R. L. Introduction to Nuclear Engineering. (Second Edition). Englewood Cliffs, N. J.: Prentice-Hall, 1961.
24. Lettau, H. "Theory of Surface-Temperature and Heat-Transfer Oscillations Near a Level Ground Surface." Transactions AGU, 32: 189 (April 1951).
25. Clark, M. and Hansen, C. F. Numerical Methods of Reactor Analysis. New York: Academic Press, 1964.
26. Meyers, G. E. Analytical Methods in Conduction Heat Transfer. New York: McGraw-Hill, 1971.

## Appendix A

### Soil Types

The soil types identified in this thesis were chosen to offer a wide range of properties. Some types may occur in the same locale while others would be mutually exclusive. Table VI lists the six soil types with their thermo-physical properties.

Table VI  
Thermo-physical Properties of Soil Types

Soil Type	Thermal Diffusivity $\alpha$ ( $\text{cm}^2/\text{sec}$ ) $\times 10^{-3}$	Thermal Conductivity k ( $\text{cal}/\text{cm sec}^{\circ}\text{K}$ ) $\times 10^{-3}$	Specific Heat c ( $\text{cal}/\text{gm}^{\circ}\text{K}$ )	Density $\rho$ ( $\text{gm}/\text{cm}^3$ )
I	3.70	2.17	0.33	1.78
II	1.20	.672		$\rho_c = 0.56$
III	2.00	.627	0.19	1.65
IV	1.90	1.70	0.53	1.67
V	2.00	0.40		$\rho_c = 0.20$
VI	2.00	2.21	0.60	1.50

The specific heat and density values were not available for soil types II and V. They are listed as products. Table VII lists the common names and the references from which the six soil types were taken.

Table VII  
Soil Type Names and References

Soil Type	Common Name	Reference
I	Sandy Clay (15% moisture)	(24:189)
II	Clayland Pasture	(24:189)
III	Quartz Sand (medium fine, dry)	(24:189)
IV	Calcerous Earth (43% water)	(6:288)
V	Soil (very dry)	(6:288)
VI	Wet Mud	(6:288)

## Appendix B

### Thermal Flux Inputs

The standard thermal spectrum relates the percent of total thermal energy emitted to the scaled elapsed time  $t/t_{\max}$  where  $t_{\max}$  is the time to the second thermal maximum. This value for a 500 KT weapon, detonated at an HOB of 5000 ft is 0.585 sec. Fig. 6 shows the calculated curve and the adjusted curve which is the result of requiring that 100% of the total thermal energy be emitted in ten seconds, as was the case in this study.

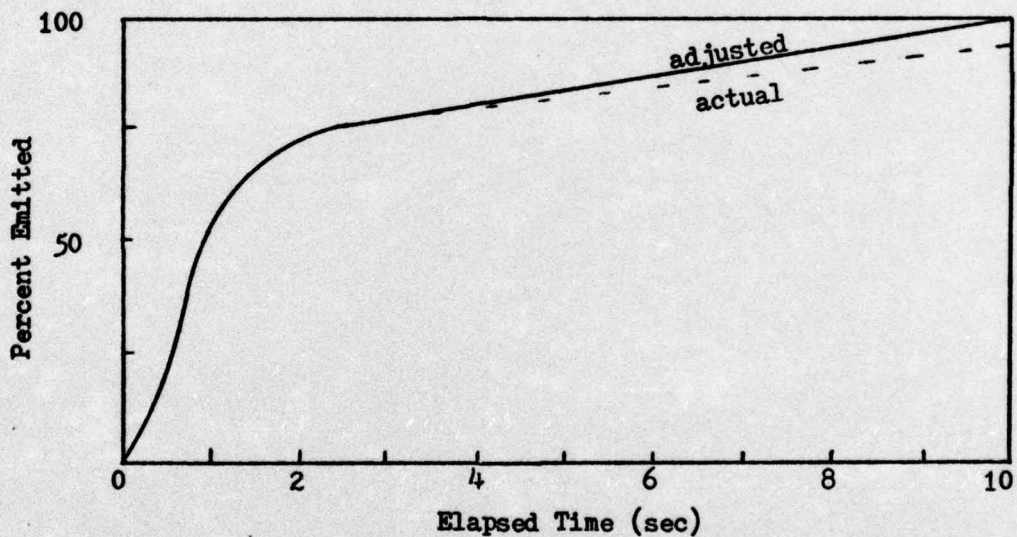


Fig. 6. Percent of Thermal Energy Emitted as a Function of Time Since Detonation

The time interval between flux inputs was chosen from an expanded version of Fig. 6 so that the rate of change from one input to another was approximately linear. After 2.5 sec of yield generation the weapon's adjusted output curve becomes linear. The number of the last

time interval before this linearization was denoted LA. From time interval LA + 1 to the end of flux input, the flux was decreased at each time interval by a constant amount called FINAGLE. This method of input was used to decrease the number of inputs to the computer program in Appendix E. Figure 7 is the resulting variation of input flux with time. The total fluence at ground zero was 700 cal/cm<sup>2</sup>.

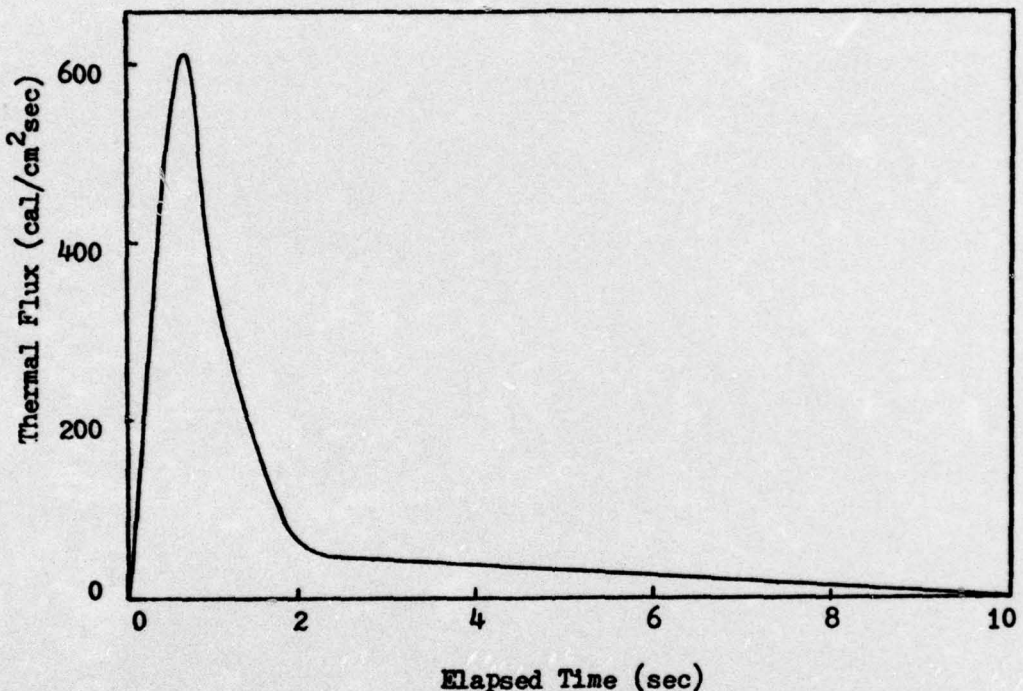


Fig. 7. Thermal Flux Input Spectrum

## Appendix C

### Spatial Mesh

The spatial mesh size in HTE4 was varied to reduce computational time. Near the surface, large gradients require closer spacing for accurate calculations. At greater depths, the lower temperature gradients allow a coarser mesh without loss of accuracy. There are 35 spatial nodes per time line as indicated in Table VIII.

Table VIII Spatial Meshing		
$\Delta x$ (cm)	# of nodes	Depth (cm)
0.2	11	0 - 2
0.5	6	2 - 5
1.0	5	5 - 10
5.0	8	10 - 50
10.0	5	50 - 100

### Time Mesh

The time spacing for the first ten seconds was kept variable to allow the flux change from one time level to the next to be kept approximately linear. The first time level was taken to be  $t = 0$  so that for  $\Delta t_1 = 0.1$  sec 101 nodes were required in the first ten seconds. If  $\Delta t_1 = 0.05$  sec, 201 nodes are required. Table IX lists the time node spacing.

Table IX  
Time Meshing

Time Increment Indicator	Time Increment (sec)	Number of Nodes	Time Period (sec)
$\Delta t_1$	variable	$(10/\Delta t_1) + 1$	0 - 10
$\Delta t_2$	1.0	90	10 - 100
$\Delta t_3$	2.0	450	100 - 1000
$\Delta t_4$	5.0	9800	1000 - 50000

## Appendix D

### Derivation of the Differenced Heat Conduction Equation and the Newton-Raphson Treatment of the Surface Temperature

The central difference operator,  $\delta$ , is defined by (Ref 25:56)

$$\delta y(x) = y(x + h/2) - y(x - h/2) \quad (26)$$

Let:  $x = i\Delta x$ ,  $t = j\Delta t$ , then  $x + h/2 = \Delta x(i + 1/2)$ . In this notation  
(time dependence suppressed)

$$\delta T_i = T_{i+1/2} - T_{i-1/2} \quad (27)$$

If  $\Delta x$  is not constant, the central difference approximation to the first spatial derivative is

$$\frac{\partial T}{\partial x} \approx \frac{T_{i+1/2} - T_{i-1/2}}{(\Delta x_i + \Delta x_{i+1})/2} \quad (28)$$

where the  $\Delta x_i$  are:  $\underbrace{\Delta x_i}_{i-1 \quad i} \quad \underbrace{\Delta x_{i+1}}_{i+1}$ .

The central difference approximation to the second derivative is

$$\frac{\partial^2 T}{\partial x^2} \approx \frac{2}{\Delta x_i + \Delta x_{i+1}} \left[ \left( \delta T_{i+1/2} / \Delta x_{i+1} \right) - \left( \delta T_{i-1/2} / \Delta x_i \right) \right] \quad (29)$$

Carrying out the indicated operations and resurrecting the suppressed time dependence, the above equation becomes

$$\frac{\partial^2 T(x, t)}{\partial x^2} \approx \frac{2(T_{i+1, j} - T_{i, j})}{\Delta x_i \Delta x_{i+1} + \Delta x_{i+1}^2} - \frac{2(T_{i, j} - T_{i-1, j})}{\Delta x_i^2 + \Delta x_i \Delta x_{i+1}} \quad (30)$$

In general, a difference equation must not be of an order higher than the derivative it replaces if instabilities are to be avoided. Thus a first forward difference operator in time was chosen, and the differenced form of the heat conduction equation, Eq (2) is

$$\frac{T_{i,j+1} - T_{i,j}}{\Delta t_j} = \frac{2\alpha(T_{i+1,j} - T_{i,j})}{\Delta x_i \Delta x_{i+1} + \Delta x_{i+1}^2} - \frac{2\alpha(T_{i,j} - T_{i-1,j})}{\Delta x_i^2 + \Delta x_i \Delta x_{i+1}} \quad (31)$$

where  $\Delta t_j$  is the time interval between nodes  $j$  and  $j+1$ , and  $\alpha$  is defined to be  $k/\rho c$ . The temperature, for points below the surface, at time line  $j+1$  in terms of the temperature at time line  $j$  is a four-point, two-level equation:

$$T_{i,j+1} = \theta_{1,i,j} T_{i+1,j} + (1 - \theta_{1,i,j} - \theta_{2,i,j}) T_{i,j} + \theta_{2,i,j} T_{i-1,j} \quad (32)$$

where:  $\theta_{1,i,j} = \frac{2\alpha \Delta t_j}{\Delta x_i \Delta x_{i+1} + \Delta x_{i+1}^2} < 1/2$

$$\theta_{2,i,j} = \frac{2\alpha \Delta t_j}{\Delta x_i^2 + \Delta x_i \Delta x_{i+1}} < 1/2.$$

The difference approximation to the surface boundary condition, Eq (3) is

$$-\frac{T_{2,i} - T_{1,i}}{\Delta x_i} = Q_{ab} - Q_{cv} - Q_{rr} \quad (33)$$

where  $Q_{ab}$  is the thermal flux absorbed at time level  $j$ . Taking all temperatures to be relative to  $T_{1,1}$  and using Eqs (3), (6), and (7),

the equation for the surface temperature is

$$T_{1,j} = \frac{\Delta x_1}{k} (TFLX_j - \sigma \epsilon T_{1,j}^4 - 2.98 \times 10^{-5} T_{1,j}^{1.33}) + T_{2,j} \quad (34)$$

Since the surface temperatures encountered are large, the surface temperature at time level  $j$  cannot be used to calculate the reradiated flux at time level  $j+1$ . The result of this method is unstable and leads to negative temperatures. The Newton-Raphson technique was used to avoid this instability (Ref 26:308).

In this method, a sliding tangent is used to find the zero of a function. The following equations of the function  $f$  refer to Fig. 8.

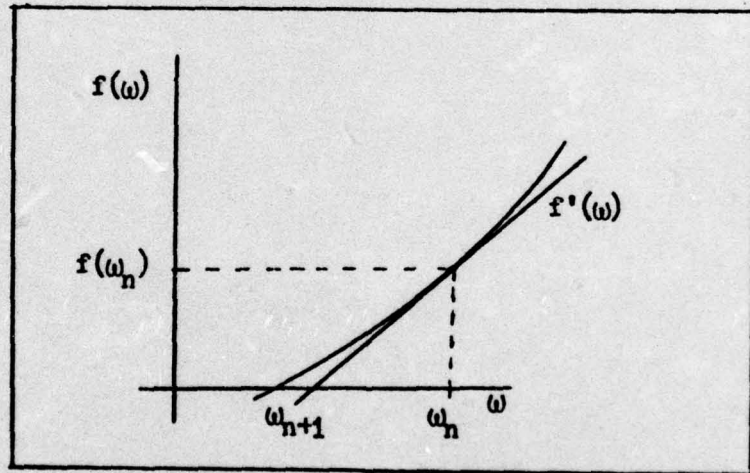


Fig. 8. Sliding Tangent

$$f'(\omega_n) = \frac{f(\omega_n) - 0}{\omega_n - \omega_{n+1}} \quad (35)$$

then  $\omega_{n+1} = \frac{(\omega_n)f'(\omega_n) - f(\omega_n)}{f'(\omega_n)} \quad (36)$

A value for  $\omega_{n+1}$  is computed from  $\omega_n$ .  $\omega_{n+1}$  is used to compute  $\omega_{n+2}$  and so on.

With the  $j$  notation suppressed, the surface temperature may be written as

$$f(T) = \frac{\Delta x_1}{k} (\sigma \epsilon T_1^4 + 2.98 \times 10^{-5} T_1^{1.33} - T_{FLX}) + T_1 - T_2 \quad (37)$$

At the  $j^{\text{th}}$  time level, the  $n+1^{\text{th}}$  iteration of the surface temperature is

$$T_{1,n+1} = \frac{3C_1 T_1^4 + C_2 (9.93 \times 10^{-6}) T_1^{1.33} + C_2 T_{FLX} + T_2}{4C_1 T_1^3 + C_2 (3.97 \times 10^{-5}) T_1^{0.33} + 1} \quad (38)$$

where  $C_1 = \Delta x_1 \sigma \epsilon / k$  and  $C_2 = \Delta x_1 / k$ .

## Appendix E

### Computer Program HTE4

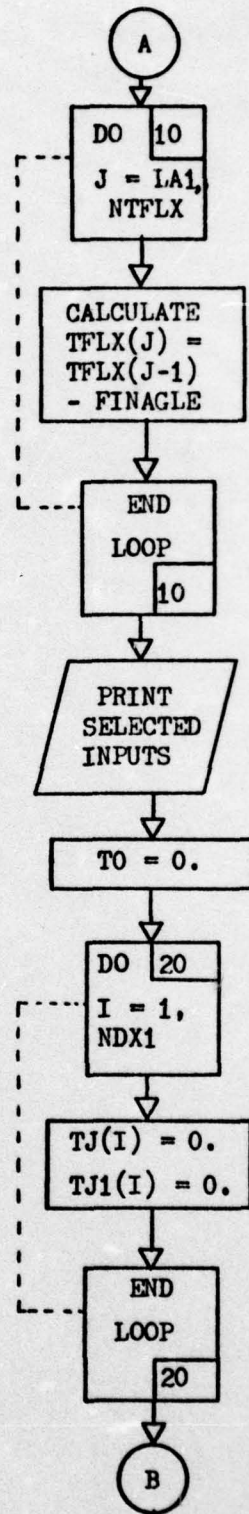
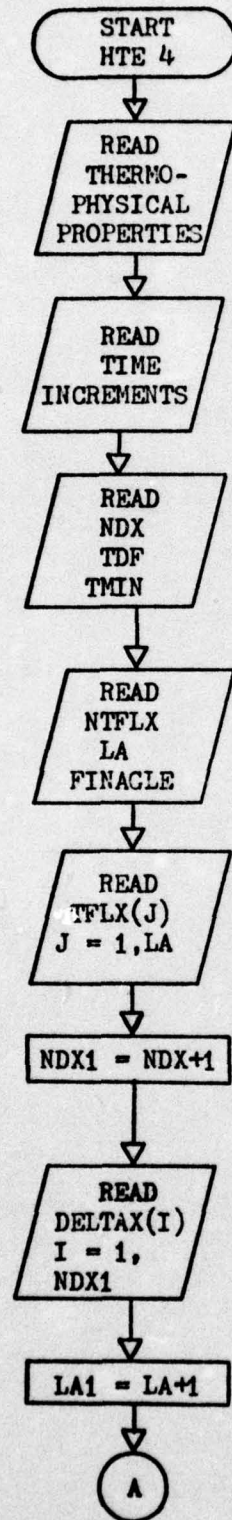
The basic calculation of temperature in HTE4 involves the following:

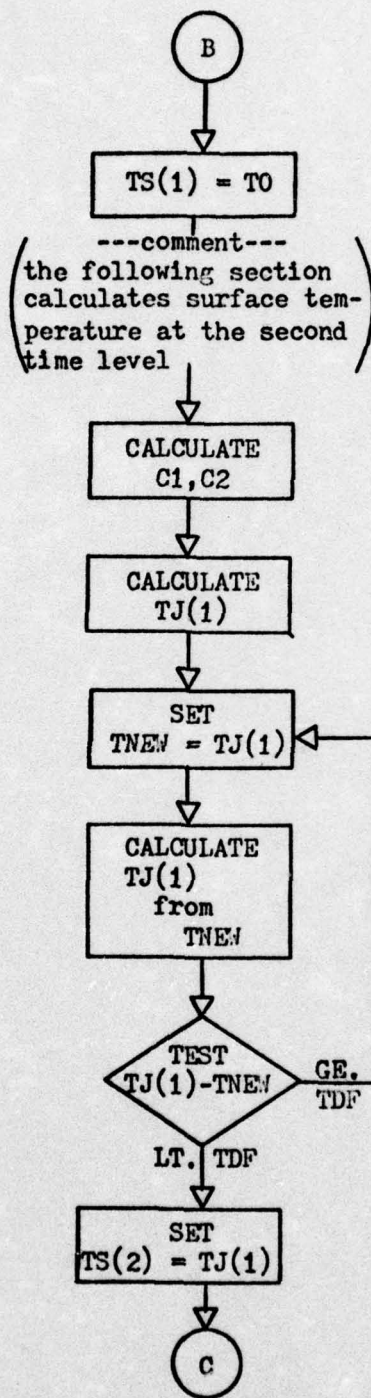
1. Calculating the values of  $R_{1,j}$  and  $R_{2,j}$  for the time increment in use
2. Calculating the subsurface temperatures using the differenced heat conduction equation
3. Calculation of the surface temperature based on flux input, convective losses, radiative losses, and the value of the temperature, computed in step 2, of the first subsurface node
4. Iteration of the surface temperature to convergence.

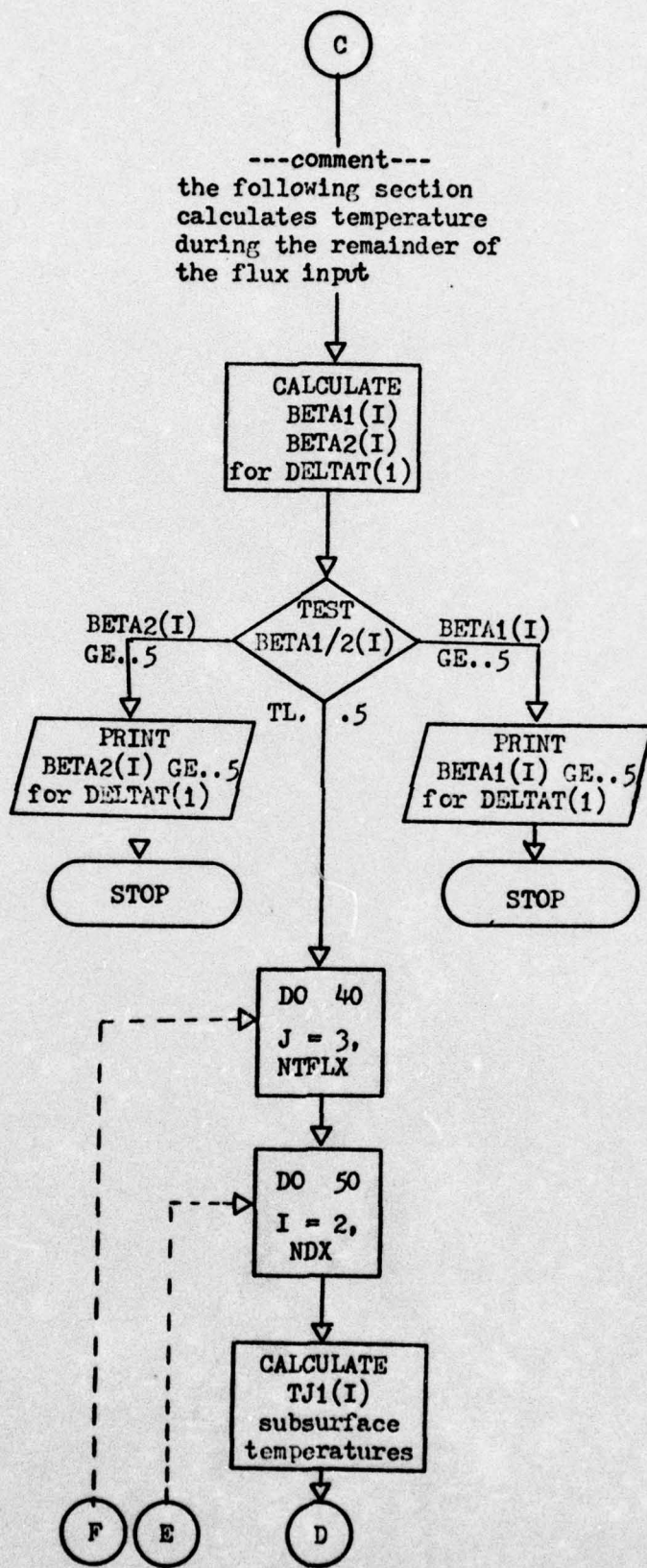
Throughout the program, J is the time index and I is the spatial index. The parameters  $C_1$  and  $C_2$ , defined in Appendix D, were used to reduce the physical space required to write out the surface temperature equation. Flux input begins at time level two, and the choice of 1000 °K as a beginning temperature for iteration is arbitrary.

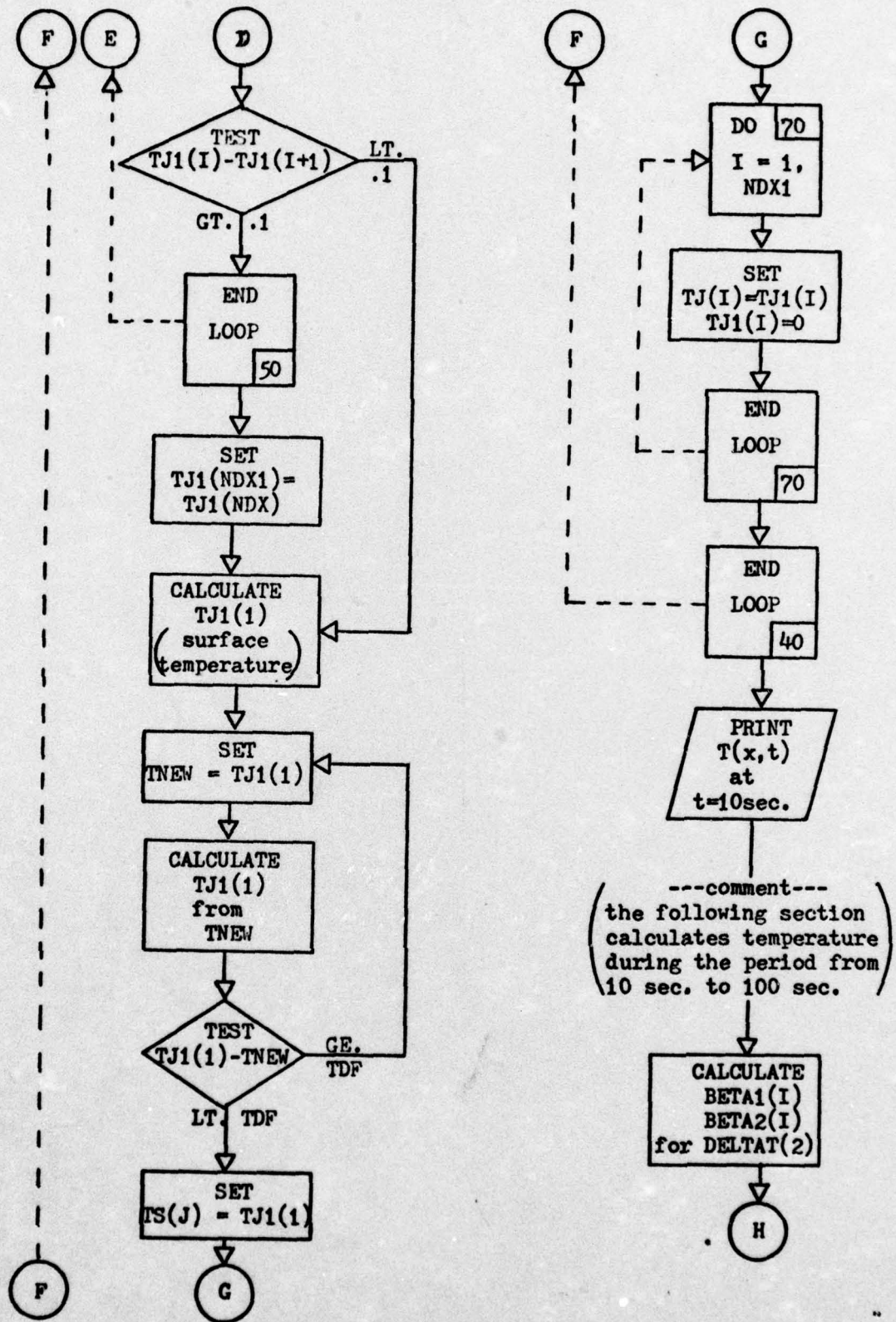
The program was written in Fortran for use on a CDC 6600 computer.

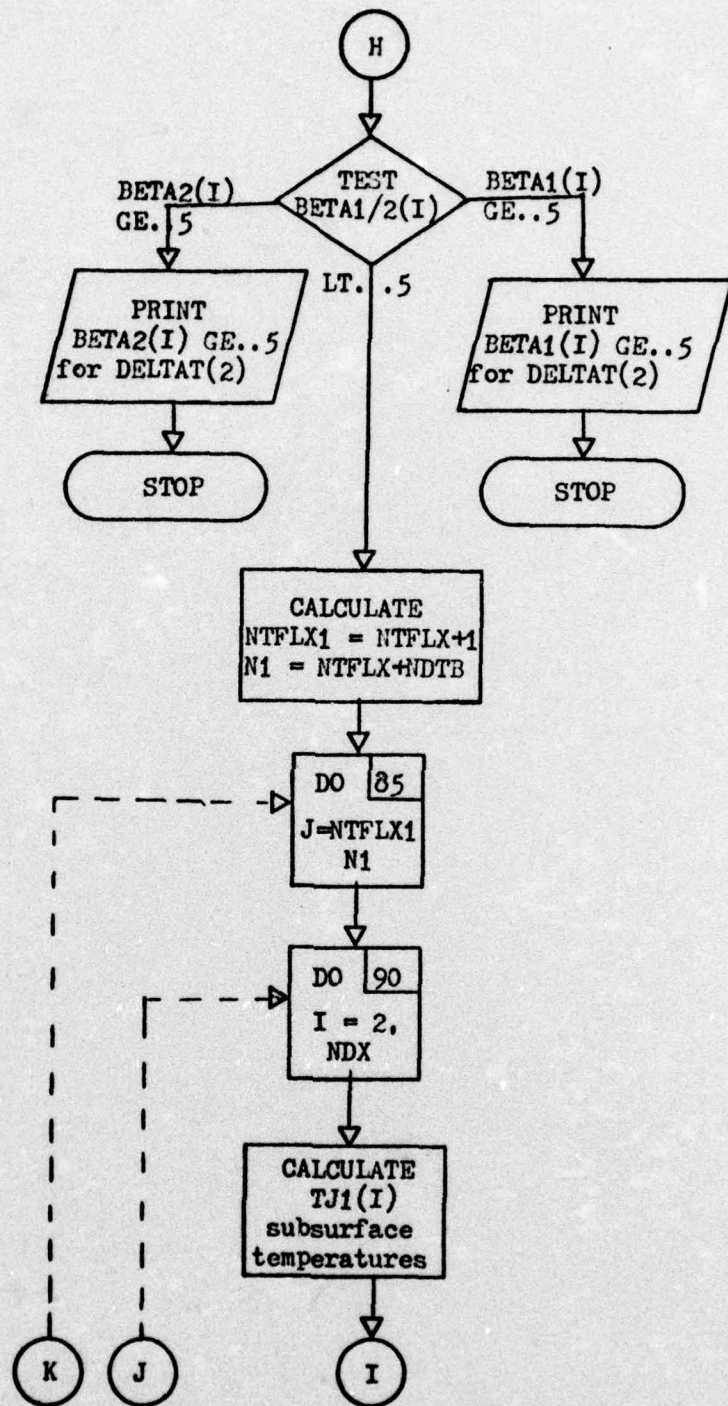
Flow Chart: HTE4

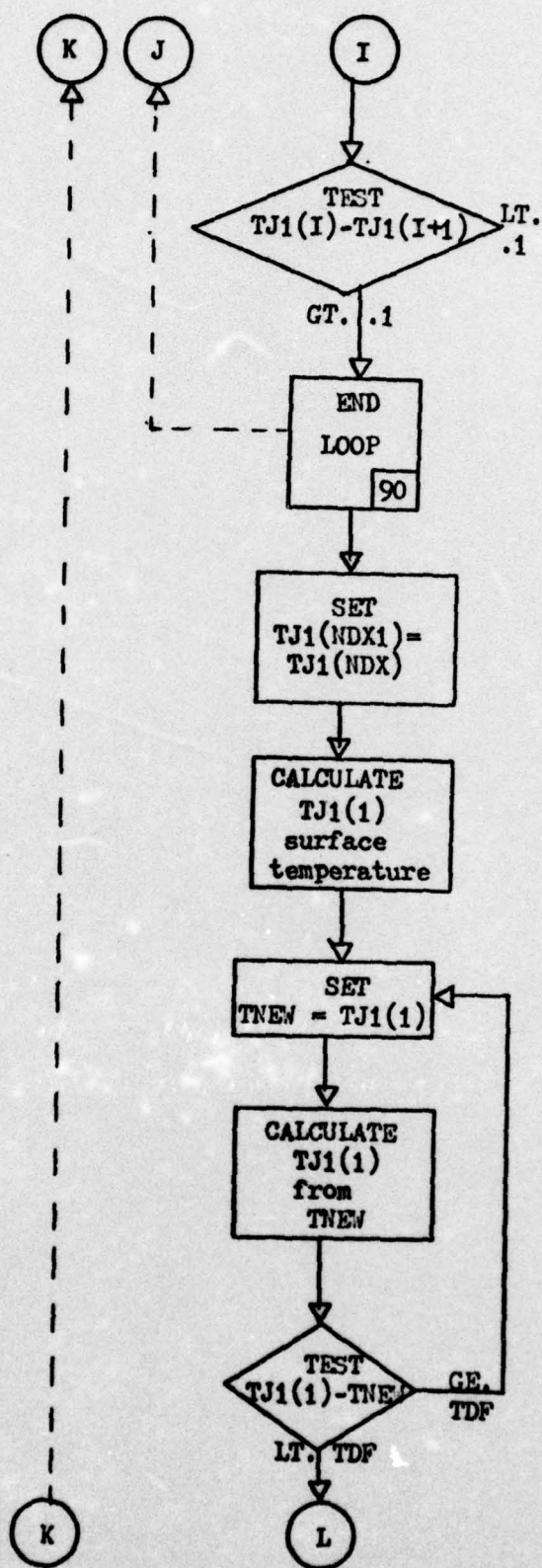


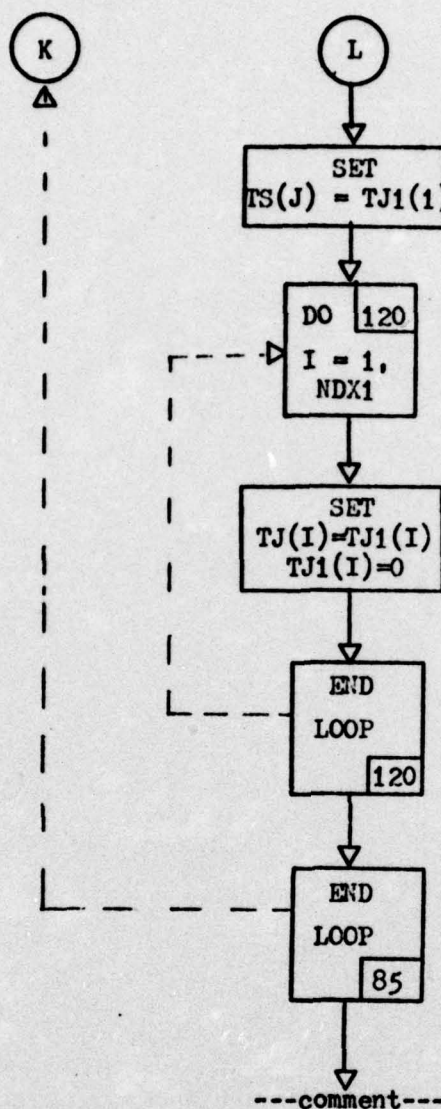












---comment---

temperature calculations from 100 to 1000 and from 1000 to 50,000 sec are similar to the preceding section. DELTAT(3), DELTAT(4), NDTC, and NDTD are used to calculate BETA. The remainder of the program is output control for the temperature readouts. As it is listed, it is valid for DELTAT(1) of 0.1 or 0.05 sec.

END HTE4

Glossary: HTE4

GLOSSARY OF TERMS USED IN THE PROGRAM HTE4-CYCLE 5

ALPHA - THERMAL DIFFUSIVITY (CM\*\*2/SEC)

BETA1(I) - DIMENSIONLESS PARAMETERS IN THE HEAT CONDUCTION EQUATION. THEY ARE FUNCTIONS OF DELTAX(I), DELTAX(I+1), ALPHA, AND DELTAT(J).

DELTAT1 - TIME INTERVAL (SEC) DURING FLUX INPUT

DELTAT2

DELTAT3 - TIME INCREMENTS (SEC) OF INCREASING SIZE WHICH ARE USED TO DECREASE COMPUTATION TIME

EPSILON - THE EMISSIVITY OF THE SURFACE

FINABLE - LINEAR FLUX CHANGE INCREMENT

DELTAX(I) - DISTANCE OF THE I-TH SPATIAL NODE FROM THE PRECEDING NODE

K - THERMAL CONDUCTIVITY (CAL/CM SEC-DEG K)

LA - LAST THERMAL FLUX INPUT BEFORE INPUT FLUX BECOMES LINEAR

N1-V15

M1-M3 - COUNTERS USED TO PRINT SURFACE TEMPERATURES AT THE INDICATED POINTS IN TIME

NDT1 - NUMBER OF TIME INTERVALS OF SIZE DELTAT1

NDT2 - NUMBER OF TIME INTERVALS OF SIZE DELTAT2

NDT3 - NUMBER OF TIME INTERVALS OF SIZE DELTAT3

NDT4 - NUMBER OF TIME INTERVALS OF SIZE DELTAT4

NDX - NUMBER OF DEPTH INTERVALS

NTFLX - NUMBER OF THERMAL FLUX INPUTS

SE - PRODUCT OF THE STEFAN BOLTZMAN CONSTANT AND THE  
EMISSIVITY OF THE SURFACE (CAL/CM\*\*2-SEC-DEG K\*\*4)

TDF - DIFFERENCE BETWEEN SUCCESSIVE ITERATIONS OF THE  
SURFACE TEMPERATURE, BELOW WHICH ITERATIONS  
ARE TERMINATED

TELX(J) - THERMAL FLUX AT TIME LINE J (CAL/CM\*\*2-SEC)

TJ(I) - AN ARRAY FOR THE TEMPORARY STORAGE OF  
THE VALUES OF T(I,J) AT TIME LINE J

TJ1(T) - AN ARRAY FOR THE TEMPORARY STORAGE OF  
THE VALUES OF T(I,J+1) AT TIME LEVEL J+1

TMIN - SURFACE TEMPERATURE (DEG-K) BELOW WHICH NO FURTHER  
CALCULATIONS ARE MADE (1,000 - 50,000 SEC)

T0 - SURFACE TEMPERATURE AT TIME ZERO (EQUAL TO 0 DEG-K)

TS(J) - THE SURFACE TEMPERATURE AT TIME LEVEL J

Program Listing: HTE4 (Grouped according to the operation performed)

```
      RFAL <
      DIMENSION TJ(35), TJ1(35), BETA1(35), BETA2(35),
      CDELTAX(35), TS(11550), TFLX(201)
      READ*, ALPHA, K, EPSILON
      READ*, DELTAT1, DELTAT2, DELTAT3, DELTAT4, NDTA, NDTB, NDTC, NDTD
      READ*, NDX, T0, TMIN
      READ*, NTFLEX, LA, FINANGLE
      READ*, (TFLX(J), J=1, LA)
      NDX1=NDX+1
      READ*, (DELTAX(I), I=1, NDX1)
      LA1=LA+1
      DO 10 J=LA1, NTFLEX
      TFLX(J)=TFLX(J-1)-FINANGLE
10    CONTINUE
      TT1=NDTA*DELTAT1
      TT2=NDTB*DELTAT2
      TT3=NDTC*DELTAT3
      TT4=NDTD*DELTAT4
      TT12=TT1+TT2
      TT123=TT1+TT2+TT3
      TT=TT1+TT2+TT3+TT4
      PRINT*
      PRINT*, "ALPHA = ", ALPHA, " CM**2/SEC"
      PRINT*, "K = ", K, " CAL/SEC*CM*DEG K"
      PRINT*, "NUMBER OF DEPTH INCREMENTS = ", NDX
      PRINT*, "TIME INCREMENTS: "
      PRINT*, "DELTAT 1 = ", DELTAT1, " SEC. FROM 0 TO ",
      CTT1, " SEC."
      PRINT*, "DELTAT 2 = ", DELTAT2, " SEC. FROM ", TT1,
      C" T0 ", TT12, " SEC."
      PRINT*, "DELTAT 3 = ", DELTAT3, " SEC. FROM ", TT12,
      C" T0 ", TT123, " SEC."
      PRINT*, "DELTAT 4 = ", DELTAT4, " SEC. FROM ", TT123,
      C" T0 ", TT, " SEC."
      LA3=LA+3
      PRINT*, "THE FIRST ", LA3, " FLUX INPJTS"
      PRINT 15, (TFLX(J), J=1, LA3)
15    FORMAT(F5.2)
      PRINT*, "SPATIAL MESH: "
      PRINT*, (DELTAX(I), I=1, NDX1)
      PRINT*
      SE=(1.35E-12)*EPSILON
      T0=0.
      DO 20 I=1, NDX1
      TJ(I)=T0
      TJ1(I)=T0
20    CONTINUE
      TS(1)=T0
      C-----TEMPERATURE CALCULATION AT SECOND TIME LEVEL-----
      C1=DELTAX(2)*SE/K
      C2=DELTAX(2)/K
```

```

      TJ(1)=(3*C1*(1000.**4)+C2*(9.93E-06)*(1000.**1.333)
      C+C2*TFLX(2)
      C+TJ(2))/(4*C1*(1000.**3)+C2*(3.97E-05)*(1000.**.333)+1.)
25      TNEW=TJ(1)
      TJ(1)=(3*C1*(TNEW **4)+C2*(9.93E-06)*(TNEW **1.333)
      C+C2*TFLX(2)
      C+TJ(2))/(4*C1*(TNEW **3)+C2*(3.97E-05)*(TNEW **.333)+1)
      IF(ABS(TJ(1)-TNEW).GE.TDF) GO TO 25
      TS(2)=TJ(1)
C-----TEMPERATURE CALCULATION DURING FLUX INPUT-----
      BETA1(1)=0.
      BETA2(1)=0.
      DO 30 I=2,NDX
      BETA1(I)=2*ALPHA*DELTAT1/(DELTAX(I)*DELTAX(I+1) +
      CDELTAX(I+1)**2)
      IF(BETA1(I).GE..5) GO TO 290
      BETA2(I)=2*ALPHA*DELTAT1/((DELTAX(I)**2)+DELTAX(I)
      C*DELTAX(I+1))
      IF(BETA2(I).GE..5) GO TO 291
30      CONTINUE
      DO 40 J=3,NTFLX
      DO 50 I=2,NDX
      TJ1(I)=BETA1(I)*TJ(I+1)+(1-BETA1(I)-BETA2(I))*TJ(I)
      C+BETA2(I)*TJ(I-1)
      IF(ABS(TJ1(I)-TJ1(I+1)).LT..1) GO TO 60
50      CONTINUE
      TJ1(NDX1)=TJ1(NDX)
50      TJ1(1)=(3*C1*(TJ(1)**4)+C2*(9.93E-06)*(TJ(1)**1.333)
      C+C2*TFLX(J)
      C+TJ1(2))/(4*C1*(TJ(1)**3)+C2*(3.97E-05)*(TJ(1)**.333)+1)
65      TNEW=TJ1(1)
      TJ1(1)=(3*C1*(TNEW **4)+C2*(9.93E-06)*(TNEW **1.333)
      C+C2*TFLX(J)
      C+TJ1(2))/(4*C1*(TNEW **3)+C2*(3.97E-05)*(TNEW **.333)+1)
      IF(ABS(TJ1(1)-TNEW).GE.TDF) GO TO 65
      TS(J)=TJ1(1)
      DO 70 I=1,NDX1
      TJ(I)=TJ1(I)
      TJ1(I)=T0
70      CONTINUE
40      CONTINUE
      PRINT*, "10 SEC: TEMPERATURE DISTRIBUTION INTO EARTH"
      DO 75 I=1,NDX1
      PRINT*, "DEPTH NODE: ",I," TEMPERATJRE = ",TJ(I)," DEG-K"
      CONTINUE
    
```

C-----TEMPERATURE CALCULATIONS FROM 10 TO 100 SEC-----

```
DO 30 I=2,NDX
  RETA1(I)=2*ALPHA*DELTAT2/(DELTAX(I)*DELTAX(I+1) +
  C*DELTAX(I+1)**2)
  IF(RETA1(I).GE..5) GO TO 292
  RETA2(I)=2*ALPHA*DELTAT2/((DELTAX(I)**2)+DELTAX(I)
  C*DELTAX(I+1))
  IF(RETA2(I).GE..5) GO TO 293
  80  CONTINUE
  NTF_X1=NTFLX+1
  1 HTE4      74/74      OPT=0 TRACE
  FTN 4.5+41

  N1=NTFLX+NDX
  DO 35 J=NTFLX1,N1
  DO 30 I=2,NDX
    TJ1(I)=BETA1(I)*TJ(I+1)+(1-BETA1(I)-BETA2(I))*TJ(I)
    C+BETA2(I)*TJ(I-1)
    IF(ABS(TJ1(I)-TJ1(I+1)).LT..1) GO TO 100
  90  CONTINUE
  TJ1(NDX1)=TJ1(NDX)
  100 TJ1(1)=(3*C1*(TJ(1)**4)+C2*(3.93E-06)*(TJ(1)**1.333)
  C+TJ1(2))/(4*C1*(TJ(1)**3)+C2*(3.97E-05)*(TJ(1)**.333)+1)
  110 TNEW=TJ1(1)
  TJ1(1)=(3*C1*(TNEW **4)+C2*(9.93E-06)*(TNEW **1.333)
  C+TJ1(2))/(4*C1*(TNEW **3)+C2*(3.97E-05)*(TNEW **.333)+1)
  IF (ABS(TJ1(1)-TNEW).GE.TDF) GO TO 110
  TS(J)=TJ1(1)
  DO 120 I=1,NDX1
    TJ(I)=TJ1(I)
  120 TJ1(I)=T0
  120 CONTINUE
  95  CONTINUE
  PRINT*, " 100 SEC TEMPERATURE DISTRIBUTION INTO EARTH"
  DO 125 I=1,NDX1
  PRINT*, "DEPTH NODE: ",I," TEMPERATJRE = ",TJ(I)," DEG-K"
  125 CONTINUE
```

```

C-----TEMPERATURE CALCULATIONS FROM 100 TO 1000 SECONDS
DO 130 T=2,NDX
  BETA1(I)=2*ALPHA*DELTAT3/(DELTAX(I)*DELTAX(I+1) +
  CDELTAX(I+1)**2)
  IF(BETA1(I).GE..5) GO TO 294
  BETA2(I)=2*ALPHA*DELTAT3/((DELTAX(I)**2)+DELTAX(I)
  C*DELTAX(I+1))
  IF(BETA2(I).GE..5) GO TO 295
130  CONTINUE
  N2=N1+1
  N3=N1+NDX
  DO 140 J=N2,N3
  DO 150 I=2,NDX
    TJ1(I)=BETA1(I)*TJ(I+1)+(1-BETA1(I)-BETA2(I))*TJ(I)
    C+BETA2(I)*TJ(I-1)
    IF(ABS(TJ1(I)-TJ1(I+1)).LT..1) GO TO 155
150  CONTINUE
    TJ1(NDX1)=TJ1(NDX)
155  TJ1(1)=(3*C1*(TJ(1)**4)+C2*(3.93E-06)*(TJ(1)**1.333)
    C+TJ1(2))/(4*C1*(TJ(1)**3)+C2*(3.97E-05)*(TJ(1)**.333)+1)
160  TNEW=TJ1(1)
    TJ1(1)=(3*C1*(TNEW **4)+C2*(3.93E-06)*(TNEW **1.333)
    C+TJ1(2))/(4*C1*(TNEW **3)+C2*(3.97E-05)*(TNEW **.333)+1)
    IF(ABS(TJ1(1)-TNEW).GE.TDF) GO TO 160
    TS(J)=TJ1(1)
    DO 170 I=1,NDX1
    TJ(I)=TJ1(I)
    TJ1(I)=T0
170  CONTINUE
140  CONTINUE
  PRINT*, " 1000 SEC: TEMPERATURE DISTRIBUTION INTO
  C EARTH"
  DO 175 I=1,NDX1
  PRINT*, "DEPTH NODE: ",I," TEMPERATURE = ",TJ(I),
  C" DEG-K"
175  CONTINUE

```

```

C-----TEMPERATURE CALCULATIONS FROM 1,000 TO 50,000 SECONDS
DO 180 I=2,NDX
  BETA1(I)=2*ALPHA*DELTAT4/(DELTAX(I)*DELTAX(I+1)
  C+DELTAX(I+1)**2)
  IF(BETA1(I).GE..5) GO TO 296
  BETA2(I)=2*ALPHA*DELTAT4/((DELTAX(I)**2)+DELTAX(I)
  C*DELTAX(I+1))
  IF(BETA2(I).GE..5) GO TO 297
180  CONTINUE
N4=N3+1
N5=N3+NDX
DO 190 J=N4,N5
DO 200 I=2,NDX
  TJ1(I)=BETA1(I)*TJ(I+1)+(1-BETA1(I)-BETA2(I))*TJ(I)
  C+BETA2(I)*TJ(I-1)
  IF(ABS(TJ1(I)-TJ1(I+1)).LT..1) GO TO 205
200  CONTINUE
  TJ1(NDX1)=TJ1(NDX)
205  TJ1(1)=(3*C1*(TJ(1)**4)+C2*(3.93E-06)*(TJ(1)**1.333)
  C+TJ1(2))/(4*C1*(TJ(1)**3)+C2*(3.97E-05)*(TJ(1)**.333)+1)
  TJ1(1)=TJ1(1)
  TJ1(1)=(3*C1*(TNEW **4)+C2*(3.93E-06)*(TNEW **1.333)
  C+TJ1(2))/(4*C1*(TNEW **3)+C2*(3.97E-05)*(TNEW **.333)+1)
  IF(1.05*(TJ1(1)-TNEW).GE.TDF) GO TO 210
  TS(J)=TJ1(1)
  IF (TS(J).LT.TMIN) GO TO 225
  DO 215 I=1,NDX1
    TJ(I)=TJ1(I)
    TJ1(I)=T0
215  CONTINUE
190  CONTINUE
  PRINT*, " 50000 SEC: TEMPERATURE DISTRIBUTION INTO
  C EARTH"
  DO 220 I=1,NDX1
    PRINT*, "DEPTH NODE: ",I," TEMPERATURE = ",TJ(I)," DEG-K"
  CONTINUE
220

```

```

C-----FIRST 2 SEC PRINTOUT IN .1 SEC INTERVALS-----
225 PRINT*
    N6=2./DELTAT1
    N7=.1/DELTAT1
    DO 230 J=1,N6,N7
    ET=(J-1)*DELTAT1
    PRINT*,ET," SEC: T = ",TS(J)
230 CONTINUE
C-----2 SEC TO 10 SEC PRINTOUT IN 1 SEC INTERVALS-----
    NR=N6+2
    N9=N7*10
    DO 240 J=N8,NTFLX,N9
    ET=(J-1)*DELTAT1
    PRINT*,ET," SEC: T = ",TS(J)
240 CONTINUE
C-----10 SEC TO 100 SEC PRINTOUT IN 10 SEC INTERVALS---
    M1=(10/DELTAT1)-9
    M2=(10/DELTAT1)+42
    M3=(10/DELTAT1)+342
    N10=NTFLX+10
    DO 250 J=N10,N1,10
    ET=(J- M1)*DELTAT2
    PRINT*,ET," SEC: T = ",TS(J)
250 CONTINUE
C-----100 SEC TO 1000 SEC PRINTOUT IN 100 SEC INTERVALS
    N11=N1+50
    DO 260 J=N11,N3,50
    ET=(J- M2)*DELTAT3
    PRINT*,ET," SEC: T = ",TS(J)
260 CONTINUE
C-----1,000 SEC TO 10,000 SEC PRINTOUT IN 1,000 SEC INTERVALS
    N12=N3+200
    N13=N3+1800
    DO 270 J=N12,N13,200
    ET=(J- M3)*DELTAT4
    PRINT*,ET," SEC: T = ",TS(J)
270 CONTINUE
C-----10,000 SEC TO 50,000 SEC PRINTOUT IN 5,000 SEC INTERVALS
    N14=N13+2000
    N15=N13+8000
    DO 280 J=N14,N15,1000
    ET=(J- M3)*DELTAT4
    PRINT*,ET," SEC: T = ",TS(J)
280 CONTINUE
    GO TO 300

```

```
290 PRINT*, "BETA1 (", I, ") IS GE. .5 FOR DELTAT1"  
291 GO TO 320  
291 PRINT*, "BETA2 (", I, ") IS GE. .5 FOR DELTAT1"  
291 GO TO 300  
292 PRINT*, "BETA1 (", I, ") IS GE. .5 FOR DELTAT2"  
292 GO TO 300  
293 PRINT*, "BETA2 (", I, ") IS GE. .5 FOR DELTAT2"  
293 GO TO 310  
294 PRINT*, "BETA1 (", I, ") IS GE. .5 FOR DELTAT3"  
294 GO TO 300  
295 PRINT*, "BETA2 (", I, ") IS GE. .5 FOR DELTAT3"  
295 GO TO 310  
296 PRINT*, "BETA1 (", I, ") IS GE. .5 FOR DELTAT4"  
296 GO TO 300  
297 PRINT*, "BETA2 (", I, ") IS GE. .5 FOR DELTAT4"  
300 STOP  
END
```

Appendix F

Computer Program HTE5

HTE5 is a short computer code designed to calculate the increase in the earth's temperature caused by a deposition of fission products. In the accompanying listing, the term  $1.23/((.1*DELTAT^*J)^{**1.2})$  represents the thermal flux input from the absorption of betas by the earth. HTE5 is similar to HTE4 and uses the differenced heat transfer equation for a constant space-time mesh. This code differs from HTE4 in that radiation by the surface is not considered. At the relatively low temperatures encountered, this omission causes a negligible effect.

Glossary: HTE5

ALPHA - THERMAL DIFFUSIVITY (CM\*\*2/SEC)

BETA DIMENSIONLESS PARAMETER IN THE HEAT CONDUCTION EQUATION.

DELTAT - TIME INTERVAL.

DELTAX - SPACE INTERVAL.

K - THERMAL CONDUCTIVITY (CAL/CM SEC-DEG K)

NDT - NUMBER OF TIME INTERVALS.

NDX - NUMBER OF DEPTH INTERVALS

TDF - DIFFERENCE BETWEEN SUCCESSIVE ITERATIONS OF THE SURFACE TEMPERATURE, BELOW WHICH ITERATIONS ARE TERMINATED

TJ(I) - AN ARRAY FOR THE TEMPORARY STORAGE OF THE VALUES OF T(I,J) AT TIME LINE J

TJ1(I) - AN ARRAY FOR THE TEMPORARY STORAGE OF THE VALUES OF T(I,J+1) AT TIME LEVEL J+1

T0 - SURFACE TEMPERATURE AT TIME ZERO ( EQUAL TO 0 DEG-K)

TS(J) - THE SURFACE TEMPERATURE AT TIME LEVEL J

Program Listing: HTE5

```
REAL K
DIMENSION TS(11111), TJ(21), TJ1(21)
PARAM, ALPHA, K
PARAM, NDX, NDT, TDF
PARAM, DELTAX, DELTAT
BETA = (ALPHA+DELTAT)/DELTAX**2
IF(BETA.GT..5) GO TO 99
TDF=DT*DELTAT
DELTAX*DELTAX
NDT1=NDT+1
NDX1=NDX+1
PRINT*, 
PRINT*, "TIME INCREMENT = ",DELTAT," SEC"
PRINT*, "NUMBER OF TIME INCREMENTS = ",NDT
PRINT*, "TOTAL TIME SPAN = ",TT," SEC"
PRINT*, "NUMBER OF DEPTH INCREMENTS = ",NDX
PRINT*, "DEPTH INCREMENT = ",DELTAX," CM"
PRINT*, "DEPTH = ",0," CM"
PRINT*, "BETA = ",BETA
PRINT*, "ALPHA = ",ALPHA," CM**2/SEC"
PRINT*, "K = ",K," CAL/SEC*CM*DEG K"
PRINT*, 
DO 10 I=1,NDX1
TJ(I)=0.
TJ1(I)=0.
10 CONTINUE
DO 40 J=2,NDT1
DO 50 I=2,NDX
TJ1(I)=BETA*TJ(I+1)+(1-2*BETA)*TJ(I)+BETA*TJ(I-1)
IF(1.23*(TJ1(I)-TJ1(I+1)).LT..1) GO TO 60
50 CONTINUE
TJ1(NDX1)=TJ1(NDX)
TJ1(1)=(DELTAX/K)*(1.23/((.1*DELTAT*J)**1.2)
C-(2.93-05)*TJ(1)**1.33)+TJ1(2)
55 TNEM=TJ1(1)
59 TJ1(1)=(DELTAX/K)*(1.23/((.1*DELTAT*J)**1.2)
C-(2.93-05)*TNEM**1.33)+TJ1(2)
```

```

TF(1)*S(TJ1(1)-T1EN),GT,TOE) GO TO 65
TS(J)=TJ1(1)
DO 70 I=1,NDX1
TJ(I)=TJ1(I)
TJ1(I)=".
70  CONTINUE
40  CONTINUE
BRTIT*
PRINT*, "TIME SINCE DEPOSITION"
DO 30 J=2,20,2
ET=J*DELTAT
PRINT*, ET, " SEC: T = ", TS(J), " DEG-K"
80  CONTINUE
DO 31 J=40,200,20
ET=J*DELTAT
*HTE5      74/74   OPT=0 TRACE          FTN
PRINT*, ET, " SEC: T = ", TS(J), " DEG-K"
91  CONTINUE
DO 32 J=400,2100,200
ET=J*DELTAT
PRINT*, ET, " SEC: T = ", TS(J), " DEG-K"
82  CONTINUE
DO 33 J=3000,10000,1000
ET=J*DELTAT
PRINT*, ET, " SEC: T = ", TS(J), " DEG-K"
83  CONTINUE
BRTIT*
PRINT*
98  GO TO 100
99  PRINT*, "BETA IS GE. .5"
100 STOP
END

```

Appendix G

DA/S Sortie - Neutron Activation Geometry

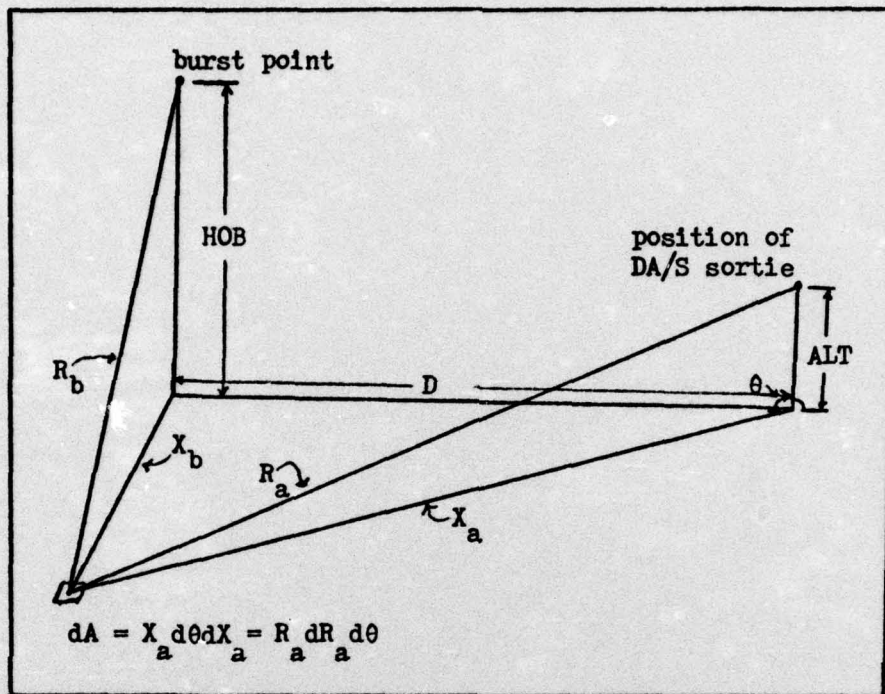


Fig. 9. DA/S Sortie - Neutron Activation Geometry

The following relations apply to Fig. 9.

$$R_b^2 = x_b^2 + HOB^2$$

$$x_b^2 = x_a^2 + D^2 - 2x_a D \cos(2\pi - \theta)$$

$$R_b^2 = x_a^2 + D^2 - 2x_a D \cos(2\pi - \theta) + HOB^2$$

$$x_a^2 = R_a^2 - ALT^2$$

$$R_b^2 = R_a^2 - ALT^2 + D^2 + HOB^2 - 2(R_a^2 - ALT^2)^{1/2} D \cos(2\pi - \theta)$$

Vita

Gordon E. Kelly was born on 23 February 1944 in Laurel, Ms. and graduated from high school in Laurel in 1961. He attended the University of Southern Mississippi from which he received the degree of Bachelor of Science in 1969. He graduated from OTS in late 1969 and completed pilot training in 1970. He flew KC-135's out of Griffiss AFB, New York for the 41<sup>st</sup> ARS until his assignment to AFIT. During the last year at Griffiss, Capt. Kelly was a Wing Officer Controller for the 416<sup>th</sup> Bomb Wing Command Post. He entered the AFIT School of Engineering in 1975.

Permanent Mailing Address: 10 Woodlawn Drive  
Laurel, Ms. 39440

**UNCLASSIFIED**

SECURITY CLASSIFICATION OF THIS PAGE (When Data Entered)

REPORT DOCUMENTATION PAGE		READ INSTRUCTIONS BEFORE COMPLETING FORM
1. REPORT NUMBER GNE/PH/76D-5	2. GOVT ACCESSION NO.	3. RECIPIENT'S CATALOG NUMBER
4. TITLE (and Subtitle) RESIDUAL SIGNATURES FROM THERMONUCLEAR AIRBURSTS		5. TYPE OF REPORT & PERIOD COVERED MS Thesis
7. AUTHOR(s) Gordon E. Kelly		6. PERFORMING ORG. REPORT NUMBER
9. PERFORMING ORGANIZATION NAME AND ADDRESS Air Force Institute of Technology (AFIT-EN) Wright-Patterson AFB, Ohio 45433		10. PROGRAM ELEMENT, PROJECT, TASK AREA & WORK UNIT NUMBERS
11. CONTROLLING OFFICE NAME AND ADDRESS SAC/XFPS HQ-SAC OAFB, NB 68113		12. REPORT DATE Dec, 1976
14. MONITORING AGENCY NAME & ADDRESS (if different from Controlling Office)		13. NUMBER OF PAGES 74
16. DISTRIBUTION STATEMENT (of this Report) Approved for public release; distribution unlimited		15. SECURITY CLASS. (of this report) UNCLASSIFIED
17. DISTRIBUTION STATEMENT (of the abstract entered in Block 20, if different from Report)		18a. DECLASSIFICATION/DOWNGRADING SCHEDULE
18. SUPPLEMENTARY NOTES <i>Approved for public release; IAW AFR 190-17</i> JERAL F. GUESS, Captain, USAF Director of Information		
19. KEY WORDS (Continue on reverse side if necessary and identify by block number) Thermonuclear Airburst Residual Signatures		
20. ABSTRACT (Continue on reverse side if necessary and identify by block number) Prompt thermal heating of the ground, fission product deposition, and neutron activation were studied as possible indicators of nuclear weapon damage levels. The time of interest was the period of approximately 13 hrs following a 500 KT low altitude, non-cratering burst. Computer calculations indicate that prompt thermal heating will produce detectable residual signatures for up to 4 hrs. Fission product depositions were found to be unusable as damage-level indicators. Calculations for (n,gamma) reactions in a soil having 2.47% Na content indicate that measurable gamma fluxes would exist throughout the period of interest.		